

# Off-Policy Correction for Actor-Critic Methods without Importance Sampling

Baturay Saglam  
Dogan C. Cicek  
Furkan B. Mutlu  
Suleyman S. Kozat

*Department of Electrical and Electronics Engineering  
Bilkent University  
06800 Bilkent, Ankara, Turkey*

BATURAY@EE.BILKENT.EDU.TR  
CICEK@EE.BILKENT.EDU.TR  
BURAK.MUTLU@EE.BILKENT.EDU.TR  
KOZAT@EE.BILKENT.EDU.TR

## Abstract

Compared to on-policy policy gradient techniques, off-policy model-free deep reinforcement learning (RL) that uses previously gathered data can improve sampling efficiency. However, off-policy learning becomes challenging when the discrepancy between the distributions of the policy of interest and the policies that collected the data increases. Although the well-studied importance sampling and off-policy policy gradient techniques were proposed to compensate for this discrepancy, they usually require a collection of long trajectories that increases the computational complexity and induce additional problems such as vanishing/exploding gradients or discarding many useful experiences. Moreover, their generalization to continuous action domains is strictly limited as they require action probabilities, which is unsuitable for deterministic policies. To overcome these limitations, we introduce a novel policy similarity measure to mitigate the effects of such discrepancy. Our method offers an adequate single-step off-policy correction without any probability estimates, and theoretical results show that it can achieve a contraction mapping with a fixed unique point, which allows “safe” off-policy learning. An extensive set of empirical results indicate that our algorithm substantially improves the state-of-the-art and attains higher returns in fewer steps than the competing methods by efficiently scheduling the learning rate in Q-learning and policy optimization.

**Keywords:** deep reinforcement learning, off-policy learning, actor-critic, importance sampling, continuous control

## 1. Introduction

Deep reinforcement learning (RL) in continuous systems still requires large amounts of data to obtain optimal policies and construct scalable agents (de Bruin et al., 2018). To improve data and sampling efficiency, agents store their experiences (transitions) in a buffer, the experience replay memory (Lin, 1992), and reuse them multiple times to perform gradient steps on their policies and value functions approximated by deep neural networks. Methods that employ experience replay are *off-policy* as the samples contained in the buffer, which are used to learn a *target* policy, are generated by a group of different policies than the one being optimized (Metelli et al., 2020). Although the past experiences of the agents may be beneficial for learning in later stages, the agent assumes that the importance of each transition is equal to each other, neglecting the fact that some of the samples may have been collected by primitive policies, such as random policies, which is referred to as *off-policy error (bias)* (Munos et al., 2016). Learning from off-policy samples can also induce

instability in learning if combined with function approximation and bootstrapping, two arguably indispensable ingredients for RL algorithms to work at scale (Zhang and Whiteson, 2022). This phenomenon is known as *the deadly triad*, and due to the combination of the mentioned entities, a sudden divergence may arise even if the policy is very close to an optimal one (Sutton and Barto, 2018, chap. 11). To mitigate the effects of the deadly triad and off-policy bias, a common approach is to disregard or completely discard transitions whose underlying distributions are uncorrelated to the distribution of the policy to be optimized, also known as *off-policy correction* (Munos et al., 2016). This is done through the relative divergence between the action probabilities generated by the current and the behavioral policies that collected the experiences, performed through importance sampling or off-policy policy gradients.

Importance sampling methods weigh the gradients of the approximated value functions according to this relative divergence using off-policy transitions sampled from the experience replay buffer (Dann et al., 2014). Importance sampling can consider temporally correlated transitions through the trajectories, e.g., (Watkins and Dayan, 1992; Degris et al., 2012; Munos et al., 2016; Harutyunyan et al., 2016; Espeholt et al., 2018), or through a single transition, e.g., (Schmitt et al., 2020). Although the widely-studied importance sampling techniques are shown to be successful in off-policy learning, these approaches introduce several issues. As the trajectory-based methods conservatively treat samples, there may be unnecessary trajectory terminations, a large amount of variance or biased action probability estimates (Munos et al., 2016; Yu et al., 2018). For single-transition methods, inaccurate importance weights are one of the broadly observed issues (Schmitt et al., 2020).

Prior to the employment of function approximators in reinforcement learning, many off-policy techniques, specifically Monte-Carlo, did not have the option to evaluate the off-policy policies in terms of the action probabilities (Harutyunyan et al., 2016). However, with the employment of value function approximators, temporal-difference (TD) (Sutton, 1988a) methods provide a continuous link between single-step and Monte-Carlo approaches through *eligibility traces* (Watkins, 1989). As the value functions in TD methods assess actions under the cumulative reward objective, they offer a direct correction to the discrepancy between the target and behavioral policies (Harutyunyan et al., 2016). Off-policy correction in terms of action probabilities via eligibility traces (Watkins, 1989) is a broadly investigated artifact for discrete action spaces (Espeholt et al., 2018; Harutyunyan et al., 2016; Munos et al., 2016; Precup et al., 2001; Degris et al., 2012; Schmitt et al., 2020). Even though actor-critic algorithms are on-policy by construction due to the Bellman optimization (Bellman, 1957), similar work for the continuous action spaces is very few, e.g., (Humayoo and Cheng, 2019; Zhang et al., 2019; Imani et al., 2018; Gu et al., 2017). Furthermore, for large action spaces, the gradients can vanish due to the product of importance weights (Han and Sung, 2019). As an environment’s observation and action spaces start to increase and more challenging tasks are introduced, the vanishing gradient problem due to importance sampling can be detrimental (Fujimoto et al., 2019). Additionally, if the continuous policy is deterministic, then off-policy correction through action probability estimates via eligibility traces is impossible by construction (Saglam et al., 2022a).

Motivated by the mentioned problems in the current importance sampling approaches and limited generalization of the off-policy correction techniques to continuous action domains, we introduce the *Actor-Critic Off-Policy Correction (AC-Off-POC)* algorithm, an alternative

single-step off-policy correction method for continuous control deep RL to overcome the effects of the deadly triad and off-policy bias when learning from off-policy data. The main contributions of this study can be summarized as follows:

- Without any strict assumptions, we derive a parameter-free, non-probabilistic policy similarity metric that measures the correlation between the behavioral policy of interest and the policies that gathered the off-policy samples. We show that this method enables us to correct the off-policy bias to achieve efficient off-policy learning in continuous control and make the standard on-policy policy gradients closer to their on-policy nature.
- By operating using a randomly sampled batch of transitions and in continuous action spaces, our algorithm prevents the high-variance build-up, vanishing gradients, and unnecessary trajectory terminations observed in traditional importance sampling methods. Therefore, the presented method can achieve a *safe* off-policy learning by constructing a contraction mapping around the discount factor with a unique fixed point.
- Our method can readily be adapted to off-policy actor-critic algorithms and experience replay sampling methods that are currently available and will be introduced in the future, which we validate through remarks and empirical results.
- We make remarks to indicate the generalizability and behavior of our approach. An extensive set of empirical studies support our claims in the provided remarks and demonstrate that, in most tasks, our algorithm improves the state-of-the-art performance and outperforms the competing off-policy correction methods in challenging OpenAI Gym (Brockman et al., 2016) continuous control tasks. Moreover, we conduct additional experiments to give insights into the introduced off-policy correction scheme and perform a sensitivity analysis based on the components that may affect off-policy learning.
- To ensure reproducibility, our source code is made publicly available at the GitHub repository<sup>1</sup>.

## 2. Related Work

Off-policy RL considers learning from experiences generated by the current or past versions of the agent’s policy. Learning from the past experiences of the policy can cause Q-values to be erroneously estimated and may degrade the performance in environments that vastly require learning from on-policy samples, i.e., data collected by the current policy of interest. Importance sampling or off-policy correction can prevent such a discrepancy in off-policy learning. This can be done through a known or estimated probability distribution of the policy (Geist and Scherrer, 2014). Initial studies in off-policy correction and importance sampling have been done by Precup et al. (2000); Watkins (1989). Before deep function approximators, basic approaches in importance sampling through eligibility traces have been studied by Precup et al. (2000). Watkins (1989) proposed an off-policy correction method

---

<sup>1</sup><https://github.com/baturaysaglam/AC-Off-POC.git>

to learn from delayed rewards. Mahmood et al. (2014) introduced a weighted importance sampling with linear function approximators. Degris et al. (2012) introduced a multi-step formulation for the expected return in terms of the importance sampling. Monte-Carlo is employed to compute the value estimates’ importance weights when the action probabilities cannot be computed due to large state and action spaces. The high variance due to the product of importance coefficients further motivated variance reduction techniques, such as the work of Precup et al. (2000), which reduces the number of steps before the bootstrapping.

With the introduction of deep function approximators in RL, Munos et al. (2016) used full returns as in the on-policy case in their RETRACE algorithm, yet Schmitt et al. (2020) shows that it introduces a zero-mean random variable at each step, yielding an increased variance in both on- and off-policy settings. The variance build-up in importance sampling is overcome by the V-trace algorithm (Espeholt et al., 2018) by trading off the variance for a biased return estimate. Differently from RETRACE, V-trace fully recovers the Monte-Carlo return under on-policy learning. Finally, Schmitt et al. (2020) presented LASER, which has been shown to eliminate the bias in the V-trace algorithm without introducing an unbounded variance. These methods were mainly introduced for discrete action spaces and have improved performance in classic Atari games and discrete control problems.

In continuous action domains, importance sampling through the probability distributions of the policies is impossible by the construction of deterministic policies (Sutton and Barto, 2018). However, Metelli et al. (2018) proposed to derive a high-confidence bound for importance weight estimates in on-policy learning. They define a surrogate objective function that optimizes the policy in an offline fashion when a new batch of trajectories is collected. Detrimental estimation bias due to the clipped importance weights to avoid the large variances is addressed by Han and Sung (2019). It is overcome by an adaptive structure that separately clips the importance weight of each action dimension for on-policy algorithms. In addition, Cicek et al. (2021) proposed an experience replay sampling algorithm that prioritizes relatively on-policy samples in training off-policy actor-critic algorithms. Their approach exhibits notable results in environments that vastly require on-policy experiences to be solved.

For off-policy learning in continuous action domains, the instability in the policy gradients due to the discrepancy between the target and behavioral policy distributions is addressed by Humayoo and Cheng (2019); Imani et al. (2018); Gu et al. (2017). Humayoo and Cheng (2019) alleviate such a discrepancy by employing a smooth variant of the relative importance sampling in their algorithm, Relative Off-Policy Actor-Critic (RIS-Off-PAC), which has a parameter  $\beta \in [0, 1]$  that controls the smoothness. Additionally, when the behavioral policy does not always aim to learn and adopt the optimal policy for the task in off-policy learning, the policy gradient theorem becomes insufficient (Imani et al., 2018). Imani et al. (2018) introduced Actor-Critic with Emphatic Weights (ACE), an off-policy policy gradient based on the emphatic weighting scheme of Sutton et al. (2016). However, the excursion objective used by Imani et al. (2018) may be misleading about the performance of the target policy. Generalized Off-Policy Actor-Critic (Geoff-PAC) (Zhang et al., 2019) solves this problem by containing a new objective for off-policy learning to compute the policy gradient of the counterfactual objective and use an emphatic approach to get an unbiased sample from this policy gradient. Moreover, Interpolated Policy Gradient (IPG) (Gu et al., 2017) merges on- and off-policy updates for actor-critic methods. They show that off-policy updates with a value function estimator can be interpolated with on-policy policy gradient updates

while the performance can still satisfy the bounds. Overall, these methods are well-known off-policy correction techniques in the control of continuous systems and have been shown to exhibit remarkable results. Thus, the introduced approach in this study is compared to these methods.

### 3. Background and Notation

Reinforcement learning considers the paradigm of an agent interacting with its environment to collect rewards. At each discrete time step  $t$ , the agent observes a state  $s$  and chooses an action  $a$ , for which it receives a reward  $r$  and observes a next state  $s'$ . In fully observable environments, the RL problem is represented by a Markov decision process (MDP), a tuple  $(\mathcal{S}, \mathcal{A}, P, \gamma)$  where  $\mathcal{S} \in \mathbb{R}^m$  and  $\mathcal{A} \in \mathbb{R}^n$  denotes the state and action spaces, respectively,  $P$  is the transition dynamics such that  $s', r \sim P(s, a)$ , and  $\gamma$  is the constant discount factor. The *return* is defined as the discounted sum of rewards  $R_t = \sum_{i=0}^{\infty} \gamma^i r_{t+i}$ , where  $\gamma$  prioritizes the short-term rewards. The goal of an agent is to find a policy  $\pi$  that maximizes the expected return:  $\mathbb{E}_{s \sim P_\pi, a \sim \pi, r \sim P}[R_0]$ , where  $P_\pi$  is the distribution over the states visited by policy  $\pi$ . Policy of an agent is stochastic if it maps states to action probabilities  $\pi : \mathcal{S} \rightarrow p(\mathcal{A})$  or deterministic if it maps states to a single action  $\pi : \mathcal{S} \rightarrow \mathcal{A}$ . There exists an action-value function (Q-function or critic) corresponding to each policy  $\pi$  that represents the expected return while following the policy after taking action  $a$  in state  $s$ , which is computed through the Bellman operator  $\mathcal{T}^\pi$  (Bellman, 1957):

$$\mathcal{T}^\pi Q^\pi(s, a) = \mathbb{E}_{r, s' \sim P, a' \sim \pi}[r + \gamma Q^\pi(s', a')].$$

The Bellman operator is a contraction for  $\gamma \in [0, 1)$  with unique fixed point  $Q^\pi(s, a)$ , i.e., the resulting error is bounded by  $\gamma$  (Bertsekas and Tsitsiklis, 1996). The optimal action-value function,  $Q^*(s, a) = \max_a Q^\pi(s, a)$ , is obtained through the greedy actions of the corresponding policy, that is, actions that yield the highest action-value.

In deep reinforcement learning, the action-value functions are modeled by deep neural networks  $Q_\theta(s, a)$ , parameterized by  $\theta$ , also known as Q-networks. The Q-network is trained by minimizing a loss  $J(\theta)$  on the TD error  $\delta$ , the difference between the network output  $Q_\theta(s, a)$  and learning target  $y$ :

$$\begin{aligned} y &:= r + \gamma Q_{\theta'}(s', a'), \\ \delta &:= y - Q_\theta(s, a), \\ J(\theta) &= \mathbb{E}_{s \sim P_\pi, a \sim \pi, r, s' \sim P}[\delta^2], \end{aligned} \tag{1}$$

where  $\theta'$  is the target network parameters of the Q-network. The usage of target networks is a practical approach in deep reinforcement learning to provide a fixed objective to optimize the network and ensure stability in the updates. The target networks are usually updated by a small proportion  $\tau$  at each step, i.e.,  $\theta' \leftarrow \tau\theta + (1 - \tau)\theta'$ , called soft-update, or periodically to exactly match the behavioral networks called hard-update.

In continuous action spaces, maximum of the action-value function over possible actions, i.e.,  $\max_a Q^\pi(s, a)$ , is intractable due to infinitely many actions. Therefore, a separate network that selects actions on the observed states is employed, called the actor network (or policy network). The deep reinforcement learning algorithms that employ actor networks

are called actor-critic methods, and they enable to control of continuous systems through the employed actor network. In actor-critic algorithms, actor networks  $\pi_\phi$ , parameterized by  $\phi$ , are optimized by a one-step gradient ascent over the policy gradient. The loss for the deterministic policies  $J_{\text{det}}(\phi)$  is based on directly maximizing the Q-value estimate of the Q-network:

$$J_{\text{det}}(\phi) = \mathbb{E}_{s \sim P_\pi} [Q_\theta(s, \pi_\phi(s))]. \quad (2)$$

To realize a differentiable loss  $J_{\text{sto}}(\phi)$ , stochastic policies employ the log-derivative trick (Williams, 1992) and scale the logarithm by the expected sum of discounted rewards while following the current policy, which the Q-network estimates:

$$J_{\text{sto}}(\phi) = \mathbb{E}_{s \sim P_\pi} [\log \pi_\phi(a|s) Q_\theta(s, a)_{a \sim \pi_\phi(\cdot|s)}]. \quad (3)$$

In off-policy deep reinforcement learning, the agent’s *behavioral* policy collects experiences and stores them into the experience replay buffer to update their Q- and actor networks. As the agents progressively learn the environment and improve their policies, the distribution of the current policy may not match the distribution corresponding to the behavioral policies that previously collected transitions, such as experiences collected by a random policy in initial steps. In this case, those experiences are *off-policy samples*, and the ones collected by the current agent’s policy are *on-policy samples*. At every update step, the agent samples a batch of transitions through a sampling algorithm that may contain on- and off-policy data:

$$(\mathbf{S}^{|\mathcal{B}| \times m}, \mathbf{A}^{|\mathcal{B}| \times n}, \mathbf{R}^{|\mathcal{B}| \times 1}, \mathbf{S}'^{|\mathcal{B}| \times m}) \sim \mathcal{B}, \quad (4)$$

where  $|\mathcal{B}|$  is the number of sampled transitions, and  $\mathbf{S}^{|\mathcal{B}| \times m}$ ,  $\mathbf{A}^{|\mathcal{B}| \times n}$ ,  $\mathbf{R}^{|\mathcal{B}| \times 1}$ ,  $\mathbf{S}'^{|\mathcal{B}| \times m}$  are the state, action, reward and next state matrices in  $\mathcal{B}$ :

$$\begin{aligned} \mathbf{S}^{|\mathcal{B}| \times m} &= \begin{bmatrix} \mathbf{s}_1^m & \mathbf{s}_2^m & \dots & \mathbf{s}_{|\mathcal{B}|}^m \end{bmatrix}^\top, \\ \mathbf{A}^{|\mathcal{B}| \times n} &= \begin{bmatrix} \mathbf{a}_1^n & \mathbf{a}_2^n & \dots & \mathbf{a}_{|\mathcal{B}|}^n \end{bmatrix}^\top, \\ \mathbf{R}^{|\mathcal{B}| \times 1} &= \begin{bmatrix} r_1 & r_2 & \dots & r_{|\mathcal{B}|} \end{bmatrix}^\top, \\ \mathbf{S}'^{|\mathcal{B}| \times m} &= \begin{bmatrix} \mathbf{s}'_1^m & \mathbf{s}'_2^m & \dots & \mathbf{s}'_{|\mathcal{B}|}^m \end{bmatrix}^\top. \end{aligned}$$

Note that we use batch or mini-batch interchangeably throughout the paper. Through batch learning, we consider that the agent optimizes its actor and critic networks using the sampled batch of transitions that do not require to be necessarily temporally correlated. Following Equation 4, the loss for the policy denoted by Equation 2 and Equation 3, and for critic

denoted by Equation 1 can be adapted to the mini-batch setting:

$$\begin{aligned} \mathbf{y}^{|\mathcal{B}|\times 1} &= \mathbf{R}^{|\mathcal{B}|\times 1} + \gamma Q_{\theta'}(\mathbf{S}'^{|\mathcal{B}|\times m}, \pi_{\phi}(\mathbf{S}'^{|\mathcal{B}|\times m})), \\ \boldsymbol{\delta}^{|\mathcal{B}|\times 1} &= \mathbf{y}^{|\mathcal{B}|\times 1} - Q_{\theta}(\mathbf{S}^{|\mathcal{B}|\times m}, \mathbf{A}^{|\mathcal{B}|\times n}) \\ J(\theta) &= \frac{\|\boldsymbol{\delta}^{|\mathcal{B}|\times 1}\|_2^2}{|\mathcal{B}|}, \end{aligned} \tag{5}$$

$$J_{\text{det}}(\phi) = \frac{1}{\mathcal{B}} \sum_{\mathcal{B}} Q_{\theta}(\mathbf{S}^{|\mathcal{B}|\times m}, \pi_{\phi}(\mathbf{S}^{|\mathcal{B}|\times m})), \tag{6}$$

$$J_{\text{sto}}(\phi) = \frac{1}{\mathcal{B}} \sum_{\mathcal{B}} \log \pi_{\phi}(\mathbf{A}^{|\mathcal{B}|\times n} | \mathbf{S}^{|\mathcal{B}|\times m}) \circ Q_{\theta}(\mathbf{S}^{|\mathcal{B}|\times m}, \mathbf{A}^{|\mathcal{B}|\times n}) |_{\mathbf{A}^{|\mathcal{B}|\times n} \sim \pi_{\phi}(\cdot | \mathbf{S}^{|\mathcal{B}|\times m})},$$

where sum operators compute the loss over the row vectors of  $\mathcal{B}$ ,  $\circ$  is the Hadamard product, and  $\|\cdot\|_2$  is the L<sub>2</sub> norm.

#### 4. Off-Policy Correction for Actor-Critic Algorithms without Importance Sampling

Our goal is to achieve more efficient off-policy learning by disregarding transitions that the distribution under which does not match the distribution of the current policy. To enable safe and efficient off-policy learning, we first aim to mitigate the effects of off-policy error induced by the data collected by divergent behavioral policies. In the following subsections, we introduce Actor-Critic Off-Policy Correction (AC-Off-POC) with deterministic and stochastic variants that measure the similarity between two policies. We show that the effect of each off-policy sample in the optimization can be corrected through the Jensen-Shannon divergence without action probability estimates under a basic multivariate Gaussian assumption on the actions. AC-Off-POC projects the similarity measure within the interval  $[0, 1]$ , where 1 indicates identical policies and 0 indicates uncorrelated ones, to weigh the losses of the actor and critic networks. We then introduce a general off-policy actor-critic framework with AC-Off-POC for continuous control and support our claims with theoretical derivations. We show that AC-Off-POC provides a safe off-policy correction through the mentioned bounded  $\gamma$ -contraction mapping. We make remarks throughout the study to emphasize specific points and findings and discuss the empirical results further.

##### 4.1 Deterministic Policies

To measure the mismatch between the distributions under the off-policy experiences and current policy, we assume that at every step  $t$ , the multi-dimensional continuous actions are samples of a multivariate Gaussian distribution that is unknown during the training. As the agent is progressively learning, each action selected by a different behavioral policy may be a sample of a different multivariate Gaussian distribution. However, each dimension in an action vector may be correlated to other dimensions. This is realistic since each dimension in action vectors often affects other dimensions (Todorov et al., 2012; Parberry, 2013). For instance, consider a continuous control task where a robot lies on the ground and tries to stand up, and the  $n$ -dimensional action space represents the angles of the robot’s joints. Intuitively, an angle of a joint may restrict or affect the motion of other joints. This implies

the correlation across the action dimensions. A multivariate probability distribution can represent such an action vector, specifically, the multivariate Gaussian distribution, for which dimensions of actions are correlated. In particular, the mean vector represents the deterministic action chosen by the policy, and the covariance matrix represents the additive exploration noise sampled from a zero-mean Gaussian distribution (Williams, 1992), which is a common practice to realize exploration in the state-of-the-art deterministic policy gradient algorithms (Lillicrap et al., 2016; Fujimoto et al., 2018; Haarnoja et al., 2018).

However, an agent’s policy may have multiple modes in some environments, for example, jumping over an obstacle or passing it by crouching in a 2D view. In such cases, the distributions under the actions selected by each policy mode will be another multivariate Gaussian. Therefore, transitions collected by each policy mode can be treated as if a different behavioral policy generated them. Hence, scenarios consisting of different policy modes still yield the made assumption.

**Assumption 1** *In off-policy learning, multivariate Gaussian distribution can represent the deterministic policies, having single or multiple modes. The mean vector represents the deterministic action chosen by the policy, and the covariance matrix represents the additive zero-mean Gaussian noise for realizing exploration.*

Off-policy correction requires a metric that measures the mismatch between the underlying distributions of the off-policy samples and the current policy to be optimized. Given the sampled batch of transitions denoted by Equation 4, and using Equation 6, the deterministic policy loss weighted by the similarity coefficient  $\lambda$  can be written as:

$$\tilde{J}_{\text{det}}(\phi) = \frac{\lambda}{|\mathcal{B}|} \sum_{\mathcal{B}} Q_{\theta}(\mathbf{S}^{|\mathcal{B}| \times m}, \pi_{\phi}(\mathbf{S}^{|\mathcal{B}| \times m})). \quad (7)$$

The weight  $\lambda$  measures the overall discrepancy of the sampled batch of transitions, which we refer to as *similarity weights* or *off-policy coefficients* throughout the manuscript. Suppose most of the behavioral policies within the sampled batch are distant from the current policy. In that case, the gradient step on the policy and Q-network parameters will be small since  $\lambda$  and loss are computed over the sampled batch. Then, using Equation 5 and Equation 7 in a similar fashion, the loss for the TD-learning becomes:

$$\tilde{J}(\theta) = \lambda \frac{\|\delta^{|\mathcal{B}| \times 1}\|_2^2}{|\mathcal{B}|}. \quad (8)$$

We now show how to derive the similarity weights  $\lambda$  for off-policy experiences. The agent samples a batch of off-policy transitions corresponding to different behavioral policies in each learning step. We know that given the states  $\mathbf{S}^{|\mathcal{B}| \times m}$ , each action in the experience replay buffer corresponds to a multivariate Gaussian distribution  $\mathcal{N}(\boldsymbol{\mu}^{1 \times n}, \boldsymbol{\Sigma}^{n \times n})$  with mean vector  $\boldsymbol{\mu}^{1 \times n}$  and covariance matrix  $\boldsymbol{\Sigma}^{n \times n}$ . To measure the similarity between the current policy and the policies that executed the off-policy transitions from the sampled batch  $\mathcal{B}$ , we first forward pass the states from  $\mathcal{B}$  through the actor network that corresponds to the current policy:

$$\hat{\mathbf{A}}^{|\mathcal{B}| \times n} = \pi_{\phi}(\mathbf{S}^{|\mathcal{B}| \times m}).$$

We now have the batch of current policy’s action decisions on the states from the off-policy transitions  $\hat{\mathbf{A}}^{|\mathcal{B}|\times n}$ , and the batch of past policies’ decisions  $\mathbf{A}^{|\mathcal{B}|\times n}$  from  $\mathcal{B}$ . Let  $\dot{\mathbf{A}}^{|\mathcal{B}|\times n}$  be the batch of numerical differences in action decisions, that is:

$$\dot{\mathbf{A}}^{|\mathcal{B}|\times n} := \mathbf{A}^{|\mathcal{B}|\times n} - \hat{\mathbf{A}}^{|\mathcal{B}|\times n}.$$

Observe that  $\dot{\mathbf{A}}^{|\mathcal{B}|\times n}$  indicates the numerical deviation between the action decisions of the current policy and previous behavioral policies of the agent that generated the sampled off-policy transitions. To construct a multivariate Gaussian distribution from the action difference batch  $\mathcal{N}(\dot{\boldsymbol{\mu}}^{1\times n}, \dot{\boldsymbol{\Sigma}}^{n\times n})$ , let:

$$\begin{aligned} \dot{\boldsymbol{\mu}}^{1\times n} &= \frac{1}{|\mathcal{B}|} \sum_{i=1}^{|\mathcal{B}|} \dot{\mathbf{A}}_i^{|\mathcal{B}|\times n}, \\ \dot{\boldsymbol{\Sigma}}^{n\times n} &= \frac{1}{|\mathcal{B}| - 1} \sum_{i=1}^{|\mathcal{B}|} (\dot{\mathbf{A}}_i^{|\mathcal{B}|\times n} - \dot{\boldsymbol{\mu}}^{1\times n})^\top (\dot{\mathbf{A}}_i^{|\mathcal{B}|\times n} - \dot{\boldsymbol{\mu}}^{1\times n}), \end{aligned} \tag{9}$$

where  $\dot{\mathbf{A}}_i^{|\mathcal{B}|\times n}$  represents the  $i^{\text{th}}$  row vector in  $\dot{\mathbf{A}}^{|\mathcal{B}|\times n}$  which corresponds to the  $i^{\text{th}}$  transition. Then, we define the dissimilarity measure as:

$$\rho = \text{JSD}(\mathcal{N}(\dot{\boldsymbol{\mu}}^{1\times n}, \dot{\boldsymbol{\Sigma}}^{n\times n}) \| \mathcal{N}(\mathbf{0}^{1\times n}, \sigma \mathbf{I}^{n\times n})), \tag{10}$$

where  $\sigma$  is the standard deviation of the exploration noise and  $\mathbf{I}^{n\times n}$  is the identity matrix. In addition, JSD denotes the Jensen-Shannon divergence, the symmetrized and smoothed version of the Kullback–Leibler (KL) divergence, defined by:

$$\begin{aligned} M &= \frac{1}{2}(P + Q), \\ \text{JSD}(P \| Q) &= \frac{1}{2} \text{KL}(P \| M) + \frac{1}{2} \text{KL}(Q \| M), \end{aligned}$$

where  $P$  and  $Q$  are random variables. We choose JSD for symmetric similarity measurement as the similarity of two policy distributions should not be assumed to be directed. Although KL-divergence is well-known for penalizing a distribution that is completely different from the distribution in interest, two policies in the same environment for the same task cannot be completely distinct (Sutton and Barto, 2018). Hence, we do not need to penalize two distinct distributions heavily.

**Remark 2** *The Jensen-Shannon divergence provides a symmetric similarity measurement between two probability distributions by using the Kullback-Leibler divergence. Moreover, KL-divergence heavily penalizes distributions that are entirely different from each other. Therefore, the smoothed version of KL-divergence, that is, the JS-divergence, should be used to measure the similarity between two behavioral policies throughout the training, as two policies in the same environment cannot be completely distinct.*

Rather than directly comparing the action difference with a zero multivariate Gaussian in Equation 10, we compute JSD using a reference matrix of zero-mean Gaussian with a

diagonal covariance matrix that contains the standard deviation of the exploration noise in the diagonal entries. Otherwise, policies closer to the current policy that executed a transition with exploration noise may be rejected as the action decisions numerically deviate from the current policy. Thus, we couple the standard deviation of the exploration noise with the reference matrix to form a parameter-free algorithm.

Naturally, if all transitions in the sampled batch match the distribution under the current policy, we have  $\rho = 0$  and  $\rho \in (0, \infty)$  otherwise. To project the similarity measure into the interval  $[0, 1]$  for bounded weights, a non-linear transformation can be applied:

$$\lambda = e^{-\rho}. \quad (11)$$

Notice that for two identical policies we have  $\lambda = 1$ , and for completely distinct policies we have  $\lambda = 0$ , making Equation 11 a similarity measure between two policies.

Intuitively, the deterministic variant of AC-Off-POC first computes the numerical difference between the actions chosen by the target and behavioral policies, then compares the difference with zero. This approach is equivalent to an implicit comparison of the distributions under the current policy and the policies that executed the off-policy transitions. However, one concern with the deterministic variant of AC-Off-POC may be that the minority of the transitions within the sampled batch may be executed by policies very similar to the current agent’s policy. Since we take the average of the action batch in computing the similarity weight, i.e., Equation 9, those transitions may be weighted by a fixed weight close to 0, which results in loss of information. We address this issue and conclude our off-policy correction scheme for deterministic policies in Remark 3, and provide an intuitive analysis on the impact of mini-batch size in Observation 1.

**Remark 3** *The deterministic variant of AC-Off-POC measures the overall discrepancy between the sampled batch of transitions and the underlying distribution of the current policy. If the distribution under most of the transitions in a sampled batch diverges from the current agent’s policy, the corresponding similarity weights will be small, or vice versa. Nevertheless, it should be expected that the policies corresponding to most of the transitions in a sampled batch must be close to the current policy since the networks in actor-critic methods are already optimized through mini-batch learning.*

**Observation 1** *Let  $|\mathcal{B}|$  and  $|\mathcal{R}|$  are the fixed mini-batch and experience replay buffer sizes used in training. If  $|\mathcal{B}| \rightarrow |\mathcal{R}|$ , then the mean indices of the sampled transitions will be 0.5 in the expectation, and the deterministic AC-Off-POC weights become slightly less than 0.5 due to the non-linear transformation. If  $|\mathcal{B}| \rightarrow 0$ , then the AC-Off-POC weights cannot be accurately estimated. Therefore, very large or small mini-batch sizes may result in poor performance.*

## 4.2 Stochastic Policies

The extension of AC-Off-POC to stochastic policies is trivial as probability distributions represent the policies. Although the known probability distributions can be directly used in the traditional importance sampling methods through eligibility traces (Watkins, 1989), they require sufficiently long trajectories executed by each policy, such as in (Espeholt et al.,

2018; Schmitt et al., 2020; Munos et al., 2016; Harutyunyan et al., 2016). Instead, stochastic AC-Off-POC can apply an off-policy correction on randomly selected off-policy transitions.

In this variant of AC-Off-POC, we do not need assumptions on the type of distribution the actions are sampled. Therefore, we can store the parameters of the policy distributions into the replay buffer. For example, suppose the stochastic policy of an agent is represented by a Beta distribution  $B(\alpha, \beta)$ . In that case, we store the parameters  $\alpha$  and  $\beta$  in the experience replay buffer and sample these parameters along with states, actions, and rewards at every update step.

At each learning step, the agent samples a batch of off-policy transitions along with the parameters that define the policy distribution:

$$(\mathbf{S}^{|\mathcal{B}|\times m}, \mathbf{A}^{|\mathcal{B}|\times n}, \mathbf{R}^{|\mathcal{B}|\times 1}, \mathbf{S}'^{|\mathcal{B}|\times m}, \alpha_1, \dots, \alpha_{|\mathcal{B}|}) \sim \mathcal{B},$$

where  $\alpha_1, \dots, \alpha_{|\mathcal{B}|}$  represent the distribution parameters for each behavioral policy that executed the transitions indexed by  $1, \dots, |\mathcal{B}|$ , respectively. Each behavioral policy  $\eta_i(\cdot)$  that executed the  $i^{\text{th}}$  transition can be represented with the corresponding distribution parameters:  $\eta_{\alpha_i}(\cdot)$ . Instead of comparing the difference batch with a reference Gaussian, we directly measure the similarity between the distribution under the current policy  $\pi(\cdot)$  and  $\eta_{\alpha_i}(\cdot)$ :

$$\begin{aligned} \rho_i &= \text{JSD}(\pi(\cdot) \parallel \eta_{\alpha_i}(\cdot)), \\ \lambda_i &= \min\left[\frac{\pi(a_i|s_i)}{\eta_{\alpha_i}(a_i|s_i)}, e^{-\rho_i}\right]. \end{aligned}$$

In the latter equation, we clip the similarity weights to obtain a  $\gamma$ -contraction mapping around the optimal Q-value, and hence, a ‘‘safe’’ off-policy correction, which we will examine in depth in the proof of Theorem 8. Note that  $\pi(\cdot)$  denotes the probability distribution of the current policy while  $\pi_\phi$  denotes the actor network. In addition, notice that we are on-policy for the  $i^{\text{th}}$  transition if  $\pi(\cdot) = \eta_{\alpha_i}(\cdot)$  and off-policy otherwise. We then construct a similarity weight vector for the sampled batch of transitions:

$$\boldsymbol{\lambda}^{|\mathcal{B}|\times 1} := [\lambda_1 \quad \lambda_2 \quad \dots \quad \lambda_{|\mathcal{B}|}]^\top.$$

Similar to Equation 7 and 8, we can derive the weighted policy and critic loss for stochastic actor-critic:

$$\tilde{J}_{\text{sto}}(\phi) = \frac{1}{\|\boldsymbol{\lambda}^{|\mathcal{B}|\times 1}\|_1} \sum_{\mathcal{B}} \lambda_i^{|\mathcal{B}|\times 1} \log \pi_\phi(\mathbf{A}^{|\mathcal{B}|\times n} | \mathbf{S}^{|\mathcal{B}|\times m}) \circ Q_\theta(\mathbf{S}^{|\mathcal{B}|\times m}, \mathbf{A}^{|\mathcal{B}|\times n}) |_{\mathbf{A}^{|\mathcal{B}|\times n} \sim \pi_\phi(\cdot | \mathbf{S}^{|\mathcal{B}|\times m})}, \quad (12)$$

$$\tilde{J}(\theta) = \frac{\|\boldsymbol{\lambda}^{|\mathcal{B}|\times 1} \circ \boldsymbol{\delta}^{|\mathcal{B}|\times 1}\|_2^2}{\|\boldsymbol{\lambda}^{|\mathcal{B}|\times 1}\|_1}, \quad (13)$$

where  $\|\cdot\|_1$  represents the  $L_1$  norm.

In the stochastic variant, each off-policy transition has a unique weight as it can be computed through the corresponding policy distribution. Thus, we compute the loss for actor and critic parameters using a weighted sum of the off-policy transitions. However, for deterministic policies, all off-policy transitions in  $\mathcal{B}$  are weighted by the same similarity weight  $\lambda$ . Therefore, the deterministic variant weighs the sampled batch through the overall

discrepancy instead of a weighted sum. As a result, the concern with the loss of information for the deterministic variant is overcome in the stochastic case. Nonetheless, the loss of information with deterministic policies can still be neglected as the sampled batch should be similar to the current policy on average (Fujimoto et al., 2019; Saglam et al., 2022a). We adapt Remark 3 to the stochastic variant of AC-Off-POC in the following.

**Remark 4** *Due to the transition-wise similarity measurement in the stochastic variant of AC-Off-POC, the off-policy correction is not affected by the mini-batch size. However, the impact of the batch size can still be observable on the underlying off-policy actor-critic algorithm, which may affect the performance of stochastic AC-Off-POC application.*

We refer to the resulting parameter-free algorithm as *Actor-Critic Off-Policy Correction (AC-Off-POC)* and provide a pseudocode in Algorithm 1. In the next section, we describe a generic off-policy actor-critic framework with AC-Off-POC, explain the generalizability of our method, and make a theoretical analysis of the contraction mapping produced by the off-policy correction coefficients  $\lambda$ .

### 4.3 Off-Policy Actor-Critic with AC-Off-POC

As discussed, trajectory-based importance sampling methods can introduce high-variance build-up or vanishing gradients. Specifically, when each importance weight in a trajectory is larger than 1, the multiplication of the weights causes a detrimental accumulated variance that can diminish the accuracy of the trajectory weight. In contrast, when the weights are closer to 0, the trajectory weight becomes nearly 0, which yields the gradients to vanish; therefore, no updates are to be performed. However, these issues cannot be observed in AC-Off-POC since our method does not require temporally correlated samples. Instead, single transitions are weighted by coefficients that can be at most 1, that is, weights of the off-policy transitions in a single update do not affect the weights in the next update. We summarize through the following remark how AC-Off-POC can overcome the mentioned issues observed in the importance sampling methods and why the introduced approach is preferable to providing off-policy corrections compared to standard importance sampling.

**Remark 5** *As a single coefficient weighs each transition, vanishing or exploding gradient problem due to the product of weights in the trajectory-based importance sampling methods does not occur in AC-Off-POC. This is also valid for the unnecessary trajectory termination issue since AC-Off-POC only considers transition-wise and temporally uncorrelated batch-wise similarities for stochastic and deterministic policies, respectively.*

One concern with the introduced approach is that the mean difference could be zero even when the behavioral policies are quite different from the current policy. Suppose that the action range is  $[-10, 10]$ , and the current policy outputs action 0, where half of the sampled past actions are -10, and the other half are 10. The fitted normal distribution will have a zero mean even though the policies differ considerably. In this particular example, the variance in the fitted normal distribution would mitigate this issue, that is, the empirical variance would be greater than the exploration noise added to the actions, and thus, the similarity weights will be small.

Another concern with the off-policy correction is that some environments may broadly require off-policy samples to be solved, for instance, transitions of a random policy can also

---

**Algorithm 1** Actor-Critic Off-Policy Correction (AC-Off-POC)

---

- 1: **Input:**  $\pi_\phi, \mathcal{B}$
  - 2: **Output:**  $\lambda \vee \boldsymbol{\lambda}^{|\mathcal{B}| \times 1}$
  - 3: **if**  $\pi$  is deterministic **then**
  - 4:   Obtain the mini-batch of transitions:  $(\mathbf{S}^{|\mathcal{B}| \times m}, \mathbf{A}^{|\mathcal{B}| \times n}, \mathbf{R}^{|\mathcal{B}| \times 1}, \mathbf{S}'^{|\mathcal{B}| \times m}) \sim \mathcal{B}$
  - 5:   Compute the current policy’s action decisions on the states within the sampled batch:  
 $\hat{\mathbf{A}}^{|\mathcal{B}| \times n} = \pi_\phi(\mathbf{S}^{|\mathcal{B}| \times m})$
  - 6:   Compute the numerical action difference batch:  $\dot{\mathbf{A}}^{|\mathcal{B}| \times n} := \mathbf{A}^{|\mathcal{B}| \times n} - \hat{\mathbf{A}}^{|\mathcal{B}| \times n}$
  - 7:   Construct the multivariate Gaussian distribution  $\mathcal{N}(\dot{\boldsymbol{\mu}}^{1 \times n}, \dot{\boldsymbol{\Sigma}}^{n \times n})$ :  

$$\dot{\boldsymbol{\mu}}^{1 \times n} = \frac{1}{|\mathcal{B}|} \sum_{i=1}^{|\mathcal{B}|} \dot{\mathbf{A}}_i^{|\mathcal{B}| \times n}, \quad \dot{\boldsymbol{\Sigma}}^{n \times n} = \frac{1}{|\mathcal{B}| - 1} \sum_{i=1}^{|\mathcal{B}|} (\dot{\mathbf{A}}_i^{|\mathcal{B}| \times n} - \dot{\boldsymbol{\mu}}^{1 \times n})^\top (\dot{\mathbf{A}}_i^{|\mathcal{B}| \times n} - \dot{\boldsymbol{\mu}}^{1 \times n})$$
  - 8:   Compute the similarity coefficient  $\lambda$ :  
 $\rho = \text{JSD}(\mathcal{N}(\dot{\boldsymbol{\mu}}^{1 \times n}, \dot{\boldsymbol{\Sigma}}^{n \times n}) \| \mathcal{N}(\mathbf{0}^{1 \times n}, \sigma \mathbf{I}^{n \times n})) \Rightarrow \lambda = e^{-\rho}$
  - 9: **else**
  - 10:   Obtain the mini-batch of transitions containing the policy distribution parameters:  
 $(\mathbf{S}^{|\mathcal{B}| \times m}, \mathbf{A}^{|\mathcal{B}| \times n}, \mathbf{R}^{|\mathcal{B}| \times 1}, \mathbf{S}'^{|\mathcal{B}| \times m}, \alpha_1, \dots, \alpha_{|\mathcal{B}|}) \sim \mathcal{B}$ .
  - 11:   Compute the similarity coefficients  $\boldsymbol{\lambda}^{|\mathcal{B}| \times 1} = [\lambda_1 \quad \lambda_2 \quad \dots \quad \lambda_{|\mathcal{B}|}]^\top$ :  
 $\rho_i = \text{JSD}(\pi(\cdot) \| \eta_{\alpha_i}(\cdot)) \Rightarrow \lambda_i = \min_{\frac{\pi(a_i | s_i)}{\eta_{\alpha_i}(a_i | s_i)}, e^{-\rho_i}}$
  - 12: **end if**
  - 13: **return**  $\lambda \vee \boldsymbol{\lambda}^{|\mathcal{B}| \times 1}$
- 

be used to improve a suboptimal policy. In such cases, an off-policy correction that filters out the on-policy samples may degrade the performance. This is addressed by Remark 2. Therefore, the AC-Off-POC weights should be near zero only when the distributions under two policies are nearly distinct, allowing beneficial off-policy samples to be included in the training. How AC-Off-POC performs this is explained in Remark 6.

**Remark 6** *In environments that vastly require off-policy transitions to be solved, AC-Off-POC can still include transitions that diverge from the current agent’s policy to an extent due to the non-linear transformation  $e^{-\rho}$  and the Jensen-Shannon divergence used in the similarity measurements, which does not heavily penalize two different distributions unless they are nearly distinct.*

Furthermore, as AC-Off-POC operates as a learning rate scheduler to adjust the contribution of each loss component with respect to off-policy samples, it can be employed in learning from a fixed data set, such as batch-constrained RL algorithms and imitation learning. By allowing off-policy transitions correlated to the distribution under the current policy, AC-Off-POC can inhibit the extrapolation error, a phenomenon caused by the mismatch between the distributions corresponding to the off-policy data collected by a different agent and the latest agent’s policy (Fujimoto et al., 2019). Thus, it can be applied to various off-policy reinforcement learning applications. However, batch constraint RL and imitation learning are not in the scope of this work as they require additional data generation modules.

Lastly, we provide an intuitive complexity analysis for our approach. First, AC-Off-POC introduces several arithmetic matrix operations and a single forward pass through the

**Algorithm 2** A General Framework for Off-Policy Actor-Critic with AC-Off-POC

- 
- 1: Initialize the agent with actor  $\pi_\phi$  and critic  $Q_\theta$  networks with parameters  $\phi, \theta$
  - 2: Initialize target and additional networks if required
  - 3: Initialize the experience replay buffer  $\mathcal{R}$
  - 4: **for** each exploration time step **do**
  - 5:   Explore the environment and collect a transition tuple  $(s, a, r, s')$
  - 6:   **if** the policy is stochastic **then**
  - 7:     Include the policy distribution parameters  $\alpha$  to the collected tuple
  - 8:   **end if**
  - 9:   Store transition tuple into  $\mathcal{R}$
  - 10: **end for**
  - 11: **for** each training iteration **do**
  - 12:   Sample a batch of transitions  $\mathcal{B}$  from  $\mathcal{R}$  by a sampling algorithm
  - 13:   Obtain the similarity weight(s):  $\lambda \vee \boldsymbol{\lambda}^{|\mathcal{B}| \times 1} = \mathbf{AC-Off-POC}(\pi_\phi, \mathcal{B})$
  - 14:   Update actor and critic networks with an off-policy actor-critic algorithm using the losses weighted by  $\lambda \vee \boldsymbol{\lambda}^{|\mathcal{B}| \times 1}$ , e.g., Equation 7, 8, 12, and 13
  - 15:   Update target networks if required
  - 16: **end for**
- 

actor network. A single forward pass consists of multiple matrix multiplications that are linear in the input size and dominates the rest of the matrix operations in AC-Off-POC. Hence, the complexity introduced here is  $\mathcal{O}(m)$ . Secondly, the most straightforward deep actor-critic algorithm employs two networks to represent the actor and critic. We know that backpropagation is also linear in the input size, having the same complexity as the forward pass if trained over a single iteration. Therefore, each learning step over a single iteration in an off-policy actor-critic algorithm takes  $\mathcal{O}(m) + \mathcal{O}(m + n)$  for the actor and critic networks, respectively. Considering the complexity introduced by AC-Off-POC is  $\mathcal{O}(m)$ , we deduce that AC-Off-POC increases the complexity of actor-critic algorithms slightly lower than 50% (at most).

We introduce a general off-policy actor-critic framework with AC-Off-POC in Algorithm 2. Moreover, the ‘‘safeness’’ of our off-policy correction method is emphasized in Corollary 9, where it is shown that the presented method can define a  $\gamma$ -contraction mapping around the optimal Q-value when the similarity weights are included in the TD(0) algorithm (Sutton, 1988b), that is, the Q-value error interval shrinks as there exists a significant similarity between behavioral policies corresponding to the sampled off-policy transitions and the policy of interest. Note that the TD(0) algorithm (the standard single-step TD-learning) without function approximation is extensively employed in RL literature to show a contraction mapping or provide a convergence guarantee since the algorithmic structures of modern off-policy deep RL algorithms primarily based on it, as used by Munos et al. (2016); Schmitt et al. (2020); Espeholt et al. (2018); Fujimoto et al. (2018).

**Definition 1** *The general operator for single-step off-policy correction of AC-Off-POC in the TD(0) algorithm (Sutton, 1988b) is defined by:*

$$\mathcal{H}Q(s, a) := Q(s, a) + \mathbb{E}_\eta[\lambda(r + \gamma \mathbb{E}_\pi Q(s', \cdot) - Q(s, a))], \quad (14)$$

for some non-negative coefficient  $\lambda \in [0, 1]$  and any behavioral policy  $\eta$  that collected the off-policy samples, where we define  $\mathbb{E}_\eta[\cdot] := \mathbb{E}_{s \sim P_\eta, a \sim \eta, r, s' \sim P}[\cdot]$  and  $\mathbb{E}_\pi Q(s, \cdot) := \sum_a \pi(a|s)Q(s, a)$ .

**Lemma 7** *The difference between  $\mathcal{H}Q$  and its fixed point  $Q^\pi$  is:*

$$\mathcal{H}Q(s, a) - Q^\pi(s, a) = \gamma \mathbb{E}_{s \sim P_\eta, a \sim \eta} [\mathbb{E}_\pi [(Q - Q^\pi)(s, \cdot)] - \lambda(Q - Q^\pi)(s, a)].$$

**Proof** See Appendix A. ■

**Theorem 8** *The operator  $\mathcal{H}$  defined in Definition 1 has a unique fixed point  $Q^\pi$ . Moreover, if for each action selected by the current policy  $a_\pi \sim \pi$  and sampled batch of transitions  $\mathcal{B} \sim \mathcal{R}$ , we have the similarity coefficient  $\lambda = \Lambda(a_\pi, \mathcal{B}) \in \min[\frac{\pi(a_\pi|s)}{\eta(a_\pi|s)}, e^{-\rho}]$  for the transition tuple  $(s, a, r, s') \in \mathcal{B}$  collected by the behavioral policy  $\eta$ . Then for any  $Q$ -function  $Q$ , we have  $\mathcal{H}$  being a  $\gamma$ -contraction mapping around  $Q^\pi$ :*

$$\|\mathcal{H}Q - Q^\pi\|_\infty \leq \gamma \|Q - Q^\pi\|_\infty,$$

where  $\|\cdot\|_\infty$  is the supremum norm.

**Proof** The proof considers stochastic policies and relies on the proof by Munos et al. (2016) on the importance sampling for several return-based off-policy algorithms. Reduction to deterministic policies is straightforward, as we will show. From Definition 1, it is trivial to observe that  $Q^\pi$  is the fixed point of the operator  $\mathcal{H}$  as:

$$\mathbb{E}_\eta[r + \gamma \mathbb{E}_\pi Q^\pi(s', \cdot) - Q^\pi(s, a)] = (\mathcal{T}^\pi Q^\pi - Q^\pi)(s, a) = 0,$$

since  $Q^\pi$  is the fixed point of the Bellman operator  $\mathcal{T}^\pi$ . From Lemma 7 and again defining  $\Delta Q := Q - Q^\pi$ , we have:

$$\begin{aligned} \mathcal{H}Q(s, a) - Q^\pi(s, a) &= \gamma \mathbb{E}_{s \sim P_\eta, a \sim \eta} [\mathbb{E}_\pi \Delta Q(s, \cdot) - \lambda \Delta Q(s, a)] \\ &= \gamma \mathbb{E}_{s \sim P_\eta} [\mathbb{E}_\pi \Delta Q(s, \cdot) - \mathbb{E}_{a_\pi, s \sim P_\eta, a \sim \eta, \mathcal{B} \sim \mathcal{R}} [\Lambda(a_\pi, \mathcal{B}) \Delta Q(s, a) | \mathcal{B}]] \\ &= \gamma \mathbb{E}_{s \sim P_\eta, \mathcal{B} \sim \mathcal{R}} [\sum_y (\pi(y|s) - \eta(y|s) \Lambda(y, \mathcal{B})) \Delta Q(s, y)]. \end{aligned}$$

To obtain non-negative probabilities in the latter equation,  $\Lambda(y, \mathcal{B}) \leq \frac{\pi(y|s)}{\eta(y|s)}$  must be satisfied. This is why we clip  $\lambda$  in the stochastic variant. For deterministic policies, we have  $\pi(y|s) = \eta(y|s) = 1$  as the policy is a many-to-one function in which there is a single action corresponding to a state with a probability of 1. Thus, the such constraint is already satisfied in the deterministic policy case since  $\lambda \in [0, 1]$ . Having  $\pi(y|s) - \eta(y|s) \Lambda(y, \mathcal{B}) \geq 0$  satisfied, we have:

$$\mathcal{H}Q(s, a) - Q^\pi(s, a) = \sum_{x, y} w_{x, y} \Delta Q(x, y),$$

which is a linear combination of  $\Delta Q(x, y)$  weighted by non-negative coefficients  $w_{x, y}$ :

$$w_{x, y} := \gamma \mathbb{E}_{s \sim P_\eta, \mathcal{B} \sim \mathcal{R}} [(\pi(y|s) - \eta(y|s) \Lambda(y, \mathcal{B})) \mathbb{I}\{s = x\}],$$

where  $\mathbb{I}(\cdot)$  is the indicator function. The sum of those coefficients over  $x$  and  $y$  is:

$$\begin{aligned} \sum_{x,y} w_{x,y} &= \gamma \mathbb{E}_{s \sim P_\eta, \mathcal{B} \sim \mathcal{R}} \left[ \sum_y \pi(y|s) - \eta(y|s) \Lambda(y, \mathcal{B}) \right] \\ &= \gamma \mathbb{E}_{a_\pi, \mathcal{B} \sim \mathcal{R}} [1 - \Lambda(a_\pi, \mathcal{B}) | \mathcal{B}] \\ &= \mathbb{E}_{a_\pi, \mathcal{B} \sim \mathcal{R}} [\gamma - \gamma \Lambda(a_\pi, \mathcal{B}) | \mathcal{B}]. \end{aligned}$$

Clearly, we have  $\sum_{x,y} w_{x,y} \leq \gamma$  since  $\Lambda(a_\pi, \mathcal{B}) \leq 1$  for  $\forall a_\pi, \mathcal{B}$ . Therefore,  $\mathcal{H}Q(s, a) - Q^\pi(s, a)$  is a sub-convex combination of  $\Delta Q(x, y)$  weighted by non-negative coefficients  $w_{x,y}$  which sum to at most  $\gamma$ . Hence,  $\mathcal{H}$  is a  $\gamma$ -contraction mapping around  $Q^\pi$ .  $\blacksquare$

**Corollary 9** *In the proof of Theorem 8, notice that the term  $\Lambda$  depends on  $(s, a) \in \mathcal{B}$ . If we let  $\xi(s, a) := \sum_{x,y} w_{x,y}$ , then we have deduced that:*

$$|\mathcal{H}Q(s, a) - Q^\pi(s, a)| \leq \xi(s, a) \|Q - Q^\pi\|_\infty.$$

Therefore,  $\xi(s, a) \in [0, \gamma]$  is a  $(s, a)$ -specific contraction coefficient, where  $\lambda = 0$  and  $\xi(s, a) = \gamma$  when there is no similarity and  $\xi(s, a)$  approaches zero when the distribution of behavioral policies that collected the samples within the sampled batch  $\mathcal{B}$  match the current policy’s distribution.

## 5. Experiments

We conduct experiments to evaluate the effectiveness of our off-policy correction approach. In Section 5.2, we present the simulation results for the comparative evaluation with different importance sampling methods and off-policy policy gradient techniques. We conduct experiments under different batch and replay memory sizes, experience replay sampling methods, and divergence measures in Section 5.3 for the sensitivity analysis of the introduced off-policy correction scheme. In addition, weights produced by AC-Off-POC are visualized and discussed in Section 5.4. We use the MuJoCo (Todorov et al., 2012) and Box2D (Parberry, 2013) benchmarks interfaced by OpenAI Gym (Brockman et al., 2016). For reproducibility, we do not modify the environment dynamics and reward functions. The computing infrastructure used to produce the reported results is summarized in our repository<sup>1</sup>.

### 5.1 Experimental Setup and Implementation

We apply our method to three baseline off-policy actor-critic methods: Deep Deterministic Policy Gradient (DDPG) (Lillicrap et al., 2016), Soft Actor-Critic (Haarnoja et al., 2018), and Twin Delayed DDPG (TD3) (Fujimoto et al., 2018). For comparative evaluation, we consider each baseline with and without AC-Off-POC, the continuous importance sampling method, RIS-Off-PAC, and off-policy policy gradient techniques, ACE, Geoff-PAC, and IPG. In the sensitivity analysis, we use experience replay sampling methods of Combined Experience Replay (CER) (Zhang and Sutton, 2017), Experience Replay Optimization (ERO) (Zha et al., 2019), and Prioritized Experience Replay (PER) (Schaul et al., 2016).

We use the stochastic variant of the SAC algorithm to show the performance improvement when stochastic AC-Off-POC is applied. Environment-specific and shared parameters of

SAC follows the tuned hyper-parameters from OpenAI Baselines3 Zoo<sup>2</sup> (Raffin, 2020). As the actions are sampled from the environment’s action space in the initial exploration steps, policy distribution parameters are not accessible for stochastic AC-Off-POC. Rather, we start storing these parameters after a multiple of the number of exploration time steps and remove the exploration transitions from the experience replay buffer. Our implementation of DDPG also closely matches the hyper-parameter setting outlined in the original paper. Unlike the proposed setting, we add 1000 exploration time steps with frozen parameters at the beginning of each training and increase the batch size from 64 to 256 for the agents to encounter more off-policy samples in each update. Moreover, we replace Ornstein–Uhlenbeck exploration noise with a zero-mean Gaussian with a standard deviation of 0.1, shown by Fujimoto et al. (2018) to be effective for exploration and to couple with the reference Gaussian distribution. To implement TD3, we use the author’s GitHub repository<sup>3</sup> that contains the fine-tuned version of the TD3 algorithm. Exact implementations of the baseline algorithms can be accessed from our code<sup>1</sup>.

The policy gradient methods ACE, Geoff-PAC, and IPG are applied to the baselines by replacing the policy gradient computation. The importance sampling method RIS-Off-PAC is directly applied on top of the baseline algorithms. We follow the original papers to implement ACE, IPG, and RIS-Off-PAC. Our implementation of Geoff-PAC is based on the code from the authors’ GitHub repository<sup>4</sup>. We follow the exact structure given in the original papers to implement CER and ERO. Additionally, the repository<sup>5</sup> is used to implement PER.

The competing algorithms introduce hyper-parameters that either control the bias-variance trade-off or the on-policyness of the updates. We use the tuned hyper-parameters provided in the original articles. In particular, we use the bias-variance trade-off value of  $v = 1$  for IPG as it is defined for actor-critic methods with corrected off-policy samples. As stated by Zhang et al. (2019), ACE is not sensitive for the bias parameter  $\lambda_1$  on OpenAI Gym benchmarks and  $\lambda_1 = 0$  can produce sufficiently good results. Hence, we set  $\lambda_1 = 0$  for ACE. For Geoff-PAC, however, we employ the tuned hyper-parameters of  $\lambda_1 = 0.7$ ,  $\lambda_2 = 0.6$ , and  $\hat{\gamma} = 0.2$  since they are reported to result in good empirical performance. Finally, for RIS-Off-PAC, we use 0.2 for the smoothing control parameter  $\beta$ . For all simulations, each algorithm is run for 1 million time steps with evaluations occurring every 1000 time steps, where an evaluation of an agent records the average reward over ten episodes in a distinct evaluation environment without exploration noise and updates. We report the average evaluation return of ten random seeds for initializing networks, simulators, and dependencies. Uniform sampling and an experience replay buffer of size 1 million are used in the comparative evaluations.

## 5.2 Comparative Evaluation

Evaluation results for the DDPG, SAC, and TD3 algorithms are reported in Figure 1, 2, and 3, respectively. As learning curves are intertwined and hard to follow for some of the environments, we also report the average of the last ten evaluation returns, i.e., where the algorithms converge, in Table 1. Note that for some of the tasks, the baseline actor-critic

<sup>2</sup><https://github.com/DLR-RM/r1-baselines3-zoo>

<sup>3</sup><https://github.com/sfujim/TD3>

<sup>4</sup><https://github.com/ShangtongZhang/DeepRL>

<sup>5</sup><https://github.com/sfujim/LAP-PAL>

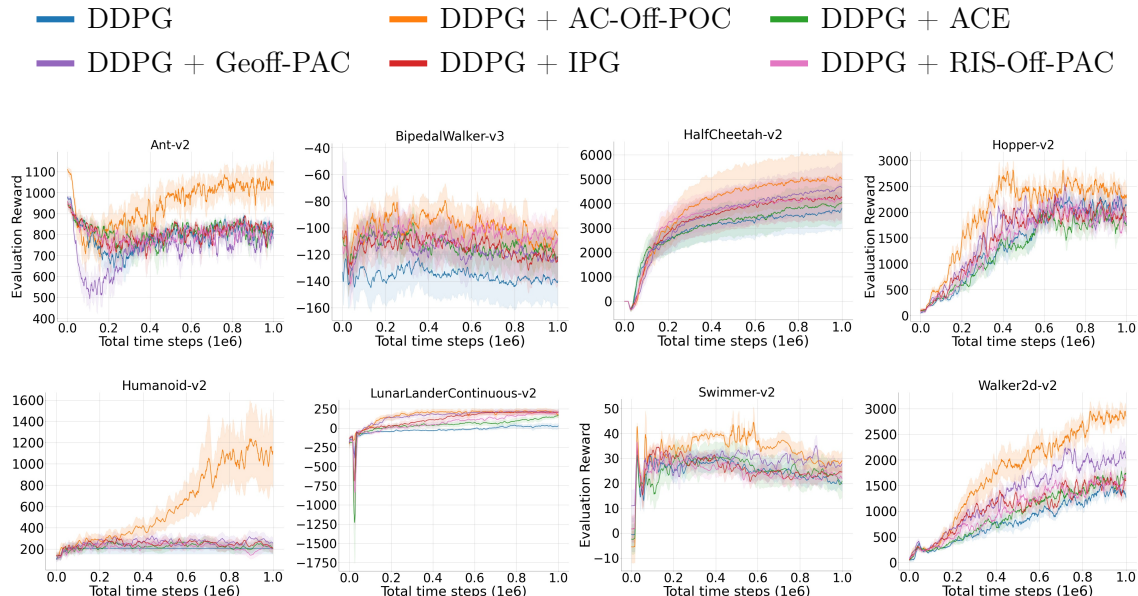


Figure 1: Evaluation curves for the set of OpenAI Gym continuous control tasks for 1 million training time steps over 10 random seeds under the DDPG algorithm. The shaded region represents a 95% confidence interval over the trials. A sliding window of size 10 smoothes the curves for visual clarity.

algorithms have worse performance than reported in the original articles. This is due to the stochasticity of the simulators and the used random seeds. Nevertheless, the performance difference between competing methods would be consistent if we used different sets of random seeds, regardless of where the baselines converge. Therefore, our comparative evaluations are fair per the standard deep RL benchmarking (Henderson et al., 2018).

We observe that both variants of AC-Off-POC significantly improve the performance of the baseline methods and either match or outperform the competing off-policy correction techniques in all of the domains tested. This shows that our off-policy correction method is scalable to many off-policy actor-critic algorithms, as previously discussed. The performance improvement obtained by AC-Off-POC is mainly more observable when the baselines are stuck at the local optima in challenging tasks, for example, Ant, BipedalWalker, Humanoid, and Swimmer. The adversity of these environments usually comes from the dimensionality of state-action spaces or internal simulation dynamics (Henderson et al., 2018). Thus, the fatal effects of off-policy samples are further amplified in these tasks, and the resulting improvement offered by an effective off-policy correction technique becomes more prominent.

Furthermore, we observe more substantial improvement by AC-Off-POC in the BipedalWalker, Hopper, Swimmer, and Walker2d environments. As shown by Henderson et al. (2018), on-policy algorithms, i.e., which learn from the data that the policy of interest collected, outperform the off-policy methods by a considerable margin in these tasks. Hence,

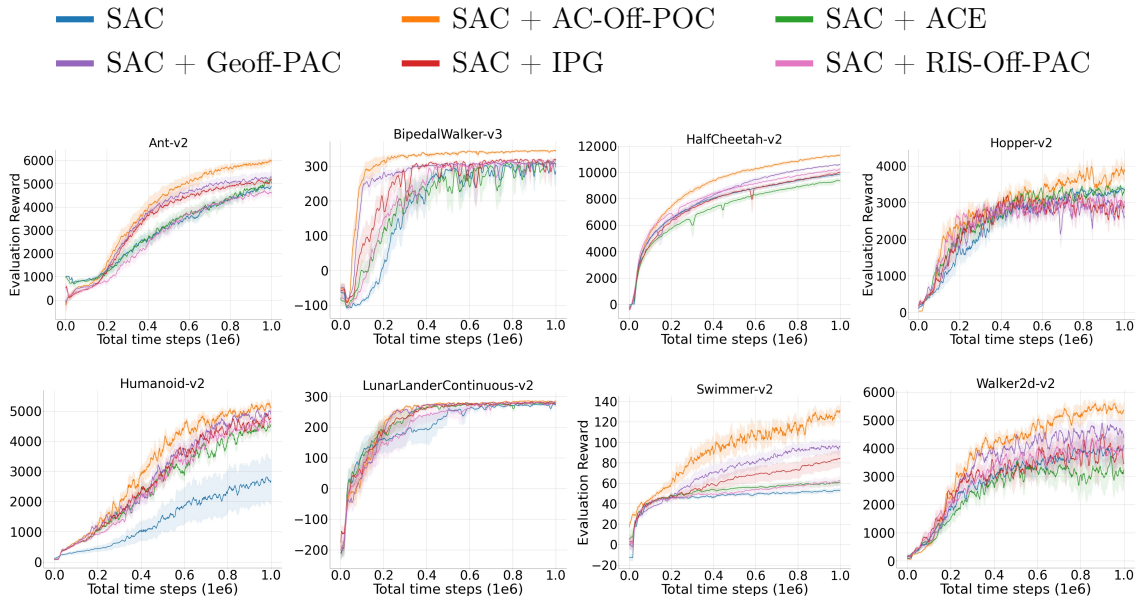


Figure 2: Evaluation curves for the set of OpenAI Gym continuous control tasks for 1 million training time steps over 10 random seeds under the SAC algorithm. The shaded region represents a 95% confidence interval over the trials. A sliding window of size 10 smoothes the curves for visual clarity.

we deduce that these environments may vastly require on-policy samples to be solved for a stable and better learning process. Hence, corrected off-policy transitions maximize the improvement compared to other environments where off-policy algorithms are often superior to the on-policy algorithms, e.g., Ant, HalfCheetah, and Humanoid. Nonetheless, we still observe improved performance in these domains. We believe that this improvement is caused by only eliminating very divergent off-policy samples collected throughout learning since the employed JSD measure assigns very low scores only to transitions that correspond to very distinct behavioral policies. Therefore, although transitions corresponding to different behavioral policies are not similar, they are still included in Q-learning and policy loss. Consequently, the latter two empirical findings validate Remarks 2 and 6.

Although the performance enhancements achieved under the SAC and TD3 algorithms remain practically the same, the overall performance improvement for stochastic policies is slightly more notable than the deterministic policies when DDPG is also considered. Nevertheless, the performance improvement on deterministic policies becomes prominent when mini-batch learning is applied as AC-Off-POC completely disregards transitions in the sampled batch. These simulation results verify Remark 3 and 4, that is, more improvement for stochastic policies is expected, yet if the distribution of the sampled transitions is similar to the distribution under the current policy on average, off-policy deterministic actor-critic methods can also be improved. These empirical results suggest that our method effectively

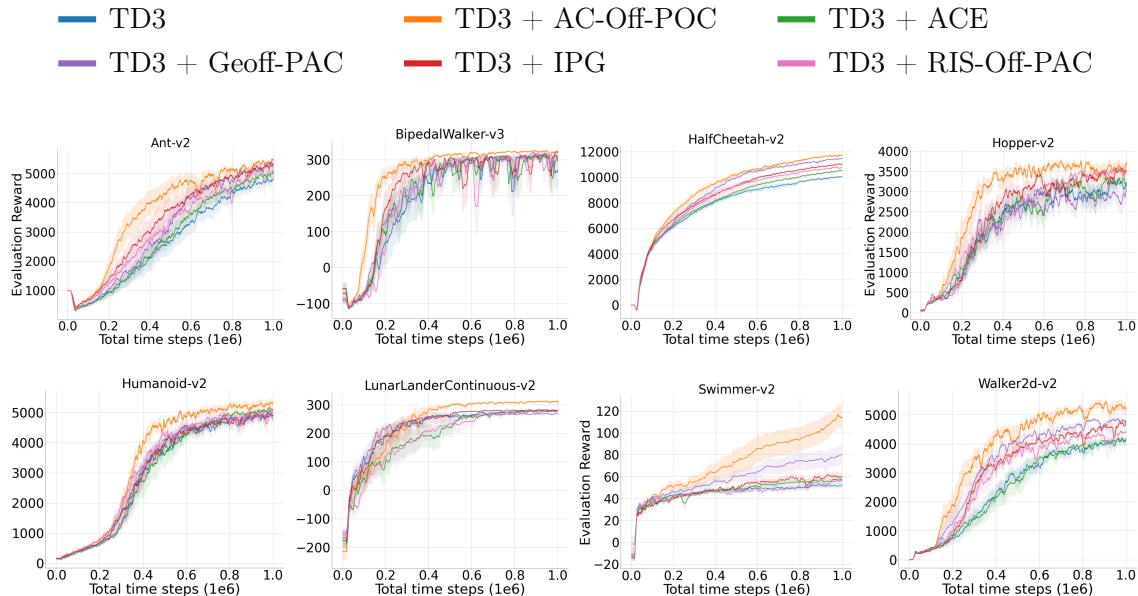


Figure 3: Evaluation curves for the set of OpenAI Gym continuous control tasks for 1 million training time steps over 10 random seeds under the TD3 algorithm. The shaded region represents a 95% confidence interval over the trials. A sliding window of size 10 smoothes the curves for visual clarity.

boosts the learning of off-policy methods and makes the agents converge to higher evaluation returns in a shorter time by disregarding highly divergent off-policy samples.

Competing methods exhibit notable stability in unstable environments such as Ant, Hopper, and Walker2d. However, the performance improvement is still not promising as they directly disregard off-policy samples through policy gradients or importance sampling. In detail, we observe that Geoff-PAC and IPG perform best with similar results among the competing algorithms, while RIS-Off-PAC obtains the worst performance, and ACE remains in the middle. As discussed, RIS-Off-PAC uses the reward function’s action-value generated from the behavioral policy to train the algorithm rather than the target policy. However, the behavioral policy that generates the action-value is usually suboptimal throughout the learning process, which yields underperformed baselines. Moreover, the empirical performance of ACE is limited to simple domains such as simple Markov chains or cart-pole balancing, as it was previously proposed for linear function approximation. Its generalization to deep function approximation, Geoff-PAC, obtains a more improved baseline performance, as expected. Although the emphatic approach in Geoff-PAC can get an unbiased sample from the policy gradient, we believe its estimation of the policy gradient is still erroneous and insufficient for optimal performance. Finally, as stated by Gu et al. (2017), IPG yields an on-policy deterministic actor-critic method when  $v = 1$  is used. Our previous discussion suggests that a complete on-policy policy gradient can completely disregard the off-policy

Method	Ant	BipedalWalker	HalfCheetah	Hopper	Humanoid	LunarLanderContinuous	Swimmer	Walker2d
DDPG	816.99 ± 165.29	-139.73 ± 36.10	3798.16 ± 1586.74	2137.20 ± 537.64	206.80 ± 105.63	26.69 ± 73.32	19.71 ± 5.90	1270.86 ± 332.23
DDPG + AC-Off-POC	<b>1052.28 ± 239.11</b>	<b>-104.79 ± 38.39</b>	<b>5012.32 ± 2155.64</b>	<b>2335.00 ± 765.72</b>	<b>1115.81 ± 641.76</b>	173.02 ± 85.59	<b>28.95 ± 7.88</b>	<b>2854.85 ± 555.45</b>
DDPG + ACE	829.96 ± 133.42	-122.38 ± 33.63	4043.05 ± 1672.13	1742.74 ± 488.32	204.14 ± 100.09	161.61 ± 58.27	20.82 ± 12.27	1742.84 ± 414.89
DDPG + Geoff-PAC	784.67 ± 133.77	-125.71 ± 36.54	4660.93 ± 1951.33	1767.06 ± 676.08	255.75 ± 115.61	<b>210.53 ± 70.60</b>	27.80 ± 5.45	2030.25 ± 625.53
DDPG + IPG	833.51 ± 88.32	-121.91 ± 39.11	4248.09 ± 1796.15	1905.45 ± 731.71	208.46 ± 84.78	207.11 ± 69.60	24.55 ± 5.47	1601.75 ± 516.69
DDPG + RIS-Off-PAC	837.10 ± 107.24	-107.97 ± 31.83	4171.61 ± 1753.42	1819.95 ± 450.00	198.50 ± 81.86	196.59 ± 66.94	21.93 ± 6.86	1644.48 ± 462.71
SAC	4864.24 ± 296.94	285.37 ± 50.74	9871.42 ± 273.98	3351.43 ± 317.07	2689.22 ± 1499.29	271.37 ± 9.82	53.11 ± 4.68	4103.54 ± 805.03
SAC + AC-Off-POC	<b>5983.03 ± 341.04</b>	<b>343.96 ± 6.93</b>	<b>11320.82 ± 262.23</b>	<b>3846.05 ± 777.89</b>	<b>5098.33 ± 529.73</b>	<b>284.83 ± 7.09</b>	<b>130.29 ± 19.46</b>	<b>5366.81 ± 819.00</b>
SAC + ACE	5019.17 ± 549.69	307.18 ± 17.98	9375.53 ± 410.10	3367.48 ± 313.79	4545.63 ± 415.48	277.18 ± 7.91	60.89 ± 5.46	3239.37 ± 1193.46
SAC + Geoff-PAC	5281.92 ± 471.66	297.24 ± 29.89	10604.40 ± 173.26	2636.44 ± 791.47	4897.81 ± 508.99	279.75 ± 9.46	96.24 ± 14.80	4367.23 ± 1217.94
SAC + IPG	5173.16 ± 274.65	318.80 ± 9.41	9993.52 ± 399.77	2906.38 ± 609.73	4768.96 ± 457.70	276.29 ± 11.56	84.20 ± 16.11	3456.34 ± 1486.13
SAC + RIS-Off-PAC	4613.55 ± 430.51	313.67 ± 12.80	10267.73 ± 325.33	3036.12 ± 534.42	4646.68 ± 459.60	276.06 ± 11.19	61.90 ± 9.43	4032.21 ± 976.43
TD3	4846.66 ± 418.23	271.77 ± 79.60	10050.95 ± 168.03	3174.56 ± 401.05	4929.35 ± 331.30	277.36 ± 5.42	52.18 ± 4.45	4107.08 ± 349.81
TD3 + AC-Off-POC	<b>5472.19 ± 276.49</b>	<b>322.38 ± 6.92</b>	<b>11735.35 ± 196.97</b>	<b>3658.85 ± 354.52</b>	<b>5297.80 ± 308.16</b>	<b>308.05 ± 15.24</b>	<b>114.02 ± 21.51</b>	<b>5219.89 ± 583.36</b>
TD3 + ACE	5064.34 ± 376.07	306.96 ± 15.10	10543.87 ± 148.98	3215.57 ± 379.31	5115.29 ± 219.01	279.49 ± 5.27	57.18 ± 5.30	4179.44 ± 267.09
TD3 + Geoff-PAC	5261.21 ± 416.70	319.52 ± 15.19	11467.90 ± 148.70	3041.78 ± 516.34	4805.35 ± 397.55	268.35 ± 6.36	80.36 ± 16.91	4795.22 ± 232.31
TD3 + IPG	5332.47 ± 367.49	295.09 ± 44.95	11064.32 ± 143.90	3524.52 ± 247.26	4908.21 ± 482.69	280.46 ± 5.32	59.94 ± 8.01	4751.56 ± 153.17
TD3 + RIS-Off-PAC	5045.43 ± 488.06	307.22 ± 16.90	10811.51 ± 166.86	3532.53 ± 128.64	5015.17 ± 340.12	278.38 ± 6.68	56.18 ± 5.13	4421.31 ± 194.74

Table 1: Average return of last 10 evaluations over 10 trials of 1 million time steps. ± captures a 95% confidence interval over the trials. Bold values represent the maximum under each baseline algorithm and environment.

samples. However, off-policy samples may sometimes be beneficial depending on the task. Therefore, we do not observe the maximal performance by IPG but AC-Off-POC.

Consequently, off-policy samples usually degrade the performance due to the underlying distribution that substantially diverges from the current agent’s policy. Nonetheless, off-policy methods may still require off-policy samples to learn the environment (Cicek et al., 2021). AC-Off-POC solves this issue by employing the Jensen-Shannon divergence, which obtains a smooth similarity measurement prior to the non-linear transformation. Its symmetric similarity measurement prevents the off-policy transitions from being heavily penalized and allows them to contribute to the learning progress even with a small proportion. Considering that the hyper-parameters introduced by the competing approaches increase the computational complexity and parameter-free AC-Off-PAC attains superior performance, we believe that our method provides significant gains over the prior work.

### 5.3 Sensitivity Analysis

As our technique is an off-policy method, batch and replay memory sizes and different experience replay sampling algorithms can considerably impact the learning. Therefore, we perform experiments on both variants of AC-Off-POC under different experience replay buffer and mini-batch sizes and experience replay sampling algorithms. We evaluate the baseline and AC-Off-POC with mini-batch sizes of 32, 256, 1024, and 2048 and the replay memory of sizes 1 million (1M) and 100,000 (100K). We also investigate the performance improvement by AC-Off-POC under the sampling algorithms of CER, ERO, and PER. The same experimental setting given in Section 5.1 is used. Unless otherwise stated, a mini-batch size of 256, replay memory of size 1 million transitions, and uniform sampling are used as the default setting.

#### 5.3.1 IMPACT OF THE MINI-BATCH SIZE

Table 2 presents the batch size sensitivity analysis over ten random seeds. First, the batch size of 256 gives the best performance for all methods in terms of both mean and confidence as they are already tuned, as outlined in the original papers of the baselines (Haarnoja et al., 2018; Fujimoto et al., 2018). For stochastic AC-Off-POC used in the SAC algorithm, we observe that the relative performance improvement by AC-Off-POC practically remains constant over different batch sizes. This is due to the transition-wise similarity measurement offered by the stochastic variant. Hence, when applied to stochastic policies, AC-Off-POC is not affected by the mini-batch learning and mini-batch size. Moreover, the mini-batch size considerably affects the batch-wise similarity measurement in the deterministic variant for TD3. For all environments, a larger batch size degrades the performance of AC-Off-POC and underperforms the baseline. Similarly, a performance drop exists for smaller batch sizes caused by the inaccurate estimation of JSD of two Gaussians with an insufficient number of samples. Overall, our sensitivity analysis on the batch size confirms Observation 1 and Remark 4.

#### 5.3.2 IMPACT OF THE EXPERIENCE REPLAY BUFFER SIZE

The impact of the replay memory sizes is reported in Table 3. When the experience replay memory size changes, we observe a significant performance variation in terms of both

Setting	HalfCheetah	Hopper	Walker2d
SAC (32)	9092.21 $\pm$ 312.47	3304.77 $\pm$ 348.16	3707.69 $\pm$ 844.41
SAC (256)	9871.42 $\pm$ 273.98	3351.43 $\pm$ 317.07	4103.54 $\pm$ 805.03
SAC (1024)	8766.95 $\pm$ 290.90	2700.17 $\pm$ 342.32	3848.68 $\pm$ 927.21
SAC (2048)	8477.68 $\pm$ 322.43	2930.11 $\pm$ 324.41	3222.36 $\pm$ 930.57
SAC + AC-Off-POC (32)	11022.58 $\pm$ 276.83	3470.82 $\pm$ 777.71	5135.93 $\pm$ 860.30
SAC + AC-Off-POC (256)	<b>11320.82 <math>\pm</math> 262.23</b>	<b>3846.05 <math>\pm</math> 777.89</b>	<b>5366.81 <math>\pm</math> 819.00</b>
SAC + AC-Off-POC (1024)	10459.58 $\pm$ 284.13	3269.79 $\pm$ 833.98	5242.90 $\pm$ 823.80
SAC + AC-Off-POC (2048)	9215.60 $\pm$ 303.78	3558.28 $\pm$ 893.85	4300.63 $\pm$ 918.97
TD3 (32)	8955.77 $\pm$ 181.85	2961.18 $\pm$ 434.44	3966.54 $\pm$ 377.57
TD3 (256)	10050.95 $\pm$ 168.03	3174.56 $\pm$ 401.05	4107.08 $\pm$ 349.81
TD3 (1024)	9963.48 $\pm$ 185.11	2847.66 $\pm$ 408.16	3881.20 $\pm$ 351.81
TD3 (2048)	8712.29 $\pm$ 194.69	2630.64 $\pm$ 455.97	4033.33 $\pm$ 351.51
TD3 + AC-Off-POC (32)	9104.90 $\pm$ 249.96	3112.20 $\pm$ 411.33	4951.56 $\pm$ 698.94
TD3 + AC-Off-POC (256)	<b>11735.35 <math>\pm</math> 196.97</b>	<b>3658.85 <math>\pm</math> 354.52</b>	<b>5219.89 <math>\pm</math> 583.36</b>
TD3 + AC-Off-POC (1024)	8791.17 $\pm$ 252.00	3126.42 $\pm$ 426.60	5040.96 $\pm$ 607.94
TD3 + AC-Off-POC (2048)	6982.50 $\pm$ 248.80	2176.53 $\pm$ 469.73	4713.68 $\pm$ 730.17

Table 2: Average return over the last 10 evaluations over 10 trials of 1 million time steps, comparing the impact of mini-batch sizes  $\{32, 256, 1024, 2048\}$ .  $\pm$  captures a 95% confidence interval over the trials. Bold values represent the maximum under each baseline algorithm and environment.

mean rewards and confidences. In the HalfCheetah environment, a smaller replay memory significantly degrades the performance under all methods. As discussed, this is caused by the environment dynamics of HalfCheetah, which usually requires off-policy samples to be efficiently solved. In all experiments, we consider First-In, First-Out (FIFO) buffer. Thus, the smaller replay memory contains more on-policy samples than the buffer of size 1 million transitions. For Hopper and Walker2d, smaller memory yields better performance which supports the evaluation results found in Section 5.2, that is, off-policy correction in these environments yields a further performance improvement compared to HalfCheetah as the policy is trained in a more on-policy fashion. When we decrease the size of the experience replay buffer, baseline SAC produces better results in HalfCheetah as AC-Off-POC further filters out the off-policy transitions that may be contained in the limited replay buffer and thus spoil the off-policy learning, which is outlined in Remark 6. Nonetheless, stochastic AC-Off-POC can still correct the off-policy samples and improve the performance of SAC in the rest of the environments. Furthermore, similar results can be found in the deterministic variant. AC-Off-POC with a smaller buffer underperforms the baseline in HalfCheetah while substantially improving the deterministic baseline algorithm in Hopper and Walker2d.

### 5.3.3 IMPACT OF DIFFERENT EXPERIENCE REPLAY SAMPLING ALGORITHMS

Table 4 shows the resulting performances under the considered sampling algorithms. We first observe that CER is superior among all the sampling methods. This is due to the most

Setting	HalfCheetah	Hopper	Walker2d
SAC (100K)	8596.65 $\pm$ 326.68	3446.68 $\pm$ 368.41	4117.61 $\pm$ 937.39
SAC (1M)	9871.42 $\pm$ 273.98	3351.43 $\pm$ 317.07	4103.54 $\pm$ 805.03
SAC + AC-Off-POC (100K)	8290.28 $\pm$ 309.43	<b>3959.37 <math>\pm</math> 744.74</b>	<b>5471.21 <math>\pm</math> 788.24</b>
SAC + AC-Off-POC (1M)	<b>11320.82 <math>\pm</math> 262.23</b>	3846.05 $\pm$ 777.89	5366.81 $\pm$ 819.00
TD3 (100K)	9343.67 $\pm$ 188.52	3200.30 $\pm$ 403.49	4183.48 $\pm$ 350.12
TD3 (1M)	10050.95 $\pm$ 168.03	3174.56 $\pm$ 401.05	4107.08 $\pm$ 349.81
TD3 + AC-Off-POC (100K)	9068.78 $\pm$ 255.80	<b>3790.57 <math>\pm</math> 494.83</b>	<b>5302.83 <math>\pm</math> 670.45</b>
TD3 + AC-Off-POC (1M)	<b>11735.35 <math>\pm</math> 196.97</b>	3658.85 $\pm$ 354.52	5219.89 $\pm$ 583.36

Table 3: Average return over the last 10 evaluations over 10 trials of 1 million time steps, comparing the impact of replay buffer sizes  $\{100000, 1000000\}$ .  $\pm$  captures a 95% confidence interval over the trials. Bold values represent the maximum under each baseline algorithm and environment.

recent collected transition, which is included in each update. Hence, all updates always occur with at least a single on-policy sample. A performance improvement can still be obtained when AC-Off-POC is applied to the baselines while sampling is performed through CER. However, AC-Off-POC slightly underperforms the baselines in the HalfCheetah environment under CER because of the discussed off-policy sample requirement. ERO performs poorly when applied to the baseline algorithms due to the internal structure of the algorithm, which is not in the scope of this work. Nevertheless, AC-Off-POC still improves ERO when applied to the baseline algorithms. In addition, PER usually underperforms when applied to an actor-critic method. This is an expected result since it was initially proposed for discrete action spaces where a single network, the Q-network, is used to select and evaluate action. Transitions with high prediction errors for Q-network are prioritized. However, in actor-critic methods, the actor network cannot be effectively trained through Bellman optimization where the prediction error for the critic is large (Saglam et al., 2022b). Although ERO and PER exhibit poor performance due to the discussed drawbacks, AC-Off-POC can still attain higher rewards. Therefore, we infer that AC-Off-POC can readily adapt to various experience replay sampling algorithms.

#### 5.3.4 IMPACT OF THE DIVERGENCE MEASURE

As previously discussed in Remark 2, we employ the Jensen-Shannon divergence in our approach, a symmetric measure of the KL-divergence, to measure the distance between two multivariate Gaussians. This is due to the asymmetric characteristics of JSD, that is, it does not penalize distributions that are very different as firmly as KL-divergence, which allows a further performance improvement in environments that usually require off-policy samples to be solved, e.g., HalfCheetah.

We test the resulting performance of AC-Off-POC when JSD is replaced with KL-divergence. These results are provided in Table 5. We obtain higher results with JSD in all of the environments. However, for the HalfCheetah environment, KL-divergence

significantly degrades the performance. As it severely penalizes transitions under which the policy distribution differs from the policy of interest, most off-policy transitions are not included in the gradient computation due to the corresponding small weights. As discussed, the HalfCheetah environment usually requires those off-policy transitions, and since the agent does not effectively use them, the performance drops. Overall, these empirical studies also verify Remark 2.

Setting	HalfCheetah	Hopper	Walker2d
SAC (uniform)	9871.42 $\pm$ 273.98	3351.43 $\pm$ 317.07	4103.54 $\pm$ 805.03
SAC (CER)	10539.72 $\pm$ 285.12	3442.93 $\pm$ 311.60	4105.39 $\pm$ 712.35
SAC (ERO)	9497.97 $\pm$ 284.17	3393.43 $\pm$ 315.16	4033.84 $\pm$ 843.72
SAC (PER)	8953.30 $\pm$ 296.70	2891.34 $\pm$ 317.16	3844.24 $\pm$ 832.49
SAC + AC-Off-POC (uniform)	<b>11320.82 <math>\pm</math> 262.23</b>	3846.05 $\pm$ 777.89	5366.81 $\pm$ 819.00
SAC + AC-Off-POC (CER)	9642.60 $\pm$ 209.10	<b>3905.79 <math>\pm</math> 760.39</b>	<b>5449.23 <math>\pm</math> 802.84</b>
SAC + AC-Off-POC (ERO)	11006.71 $\pm$ 272.90	3865.37 $\pm$ 765.77	5409.00 $\pm$ 827.40
SAC + AC-Off-POC (PER)	10388.39 $\pm$ 297.94	3493.84 $\pm$ 840.43	4402.69 $\pm$ 963.22
TD3 (uniform)	10050.95 $\pm$ 168.03	3174.56 $\pm$ 401.05	4107.08 $\pm$ 349.81
TD3 (CER)	10628.20 $\pm$ 173.55	3190.81 $\pm$ 400.69	4151.20 $\pm$ 342.95
TD3 (ERO)	9591.56 $\pm$ 168.77	3187.00 $\pm$ 403.67	4013.53 $\pm$ 361.32
TD3 (PER)	9578.80 $\pm$ 172.61	2637.58 $\pm$ 407.95	3447.57 $\pm$ 350.60
TD3 + AC-Off-POC (uniform)	<b>11735.35 <math>\pm</math> 196.97</b>	3658.85 $\pm$ 354.52	5219.89 $\pm$ 583.36
TD3 + AC-Off-POC (CER)	9851.44 $\pm$ 177.24	<b>3692.22 <math>\pm</math> 335.98</b>	<b>5367.62 <math>\pm</math> 486.86</b>
TD3 + AC-Off-POC (ERO)	11345.45 $\pm$ 205.72	3664.95 $\pm$ 352.06	5039.16 $\pm$ 589.69
TD3 + AC-Off-POC (PER)	10648.33 $\pm$ 231.66	3467.80 $\pm$ 415.79	4357.27 $\pm$ 622.60

Table 4: Average return over the last 10 evaluations over 10 trials of 1 million time steps, comparing the impact of uniform, CER, ERO, and PER sampling methods.  $\pm$  captures a 95% confidence interval over the trials. Bold values represent the maximum under each baseline algorithm and environment.

Setting	HalfCheetah	Hopper	Walker2d
SAC + AC-Off-POC (KL)	10747.20 $\pm$ 219.16	3567.88 $\pm$ 373.95	4980.37 $\pm$ 620.16
SAC + AC-Off-POC (JSD)	<b>11320.82 <math>\pm</math> 262.23</b>	<b>3846.05 <math>\pm</math> 777.89</b>	<b>5366.81 <math>\pm</math> 819.00</b>
TD3 + AC-Off-POC (KL)	10112.36 $\pm$ 200.21	3449.99 $\pm$ 362.96	4915.94 $\pm$ 612.65
TD3 + AC-Off-POC (JSD)	<b>11735.35 <math>\pm</math> 196.97</b>	<b>3658.85 <math>\pm</math> 354.52</b>	<b>5219.89 <math>\pm</math> 583.36</b>

Table 5: Average return over the last 10 evaluations over 10 trials of 1 million time steps, comparing the measures of the Jensen-Shannon divergence and KL-divergence.  $\pm$  captures a 95% confidence interval over the trials. Bold values represent the maximum under each baseline algorithm and environment.

## 5.4 Weight Analysis

We highlight that the deterministic variant of AC-Off-POC does not employ temporally correlated trajectories to compute the similarity weights as the state-of-the-art importance sampling methods compute the importance weights (Degrís et al., 2012; Munos et al., 2016; Harutyunyan et al., 2016; Watkins and Dayan, 1992; Espeholt et al., 2018), and instead, compute the weights through only randomly sampled off-policy transitions. We perform experiments to show the accuracy of the weights produced by deterministic AC-Off-POC through the experiences of an actor trained under the TD3 algorithm on the OpenAI Gym tasks HalfCheetah and Hopper, over 1 million time steps. Throughout the training, we store the transitions executed by the agent in temporal order. Then, we start by sampling the transitions with a window size of the mini-batch size centered at each transition. We compute the similarity weight  $\lambda$  for each sampled batch with the deterministic variant of AC-Off-POC. Figure 4 depicts the normalized values for time steps and similarity weights produced by AC-Off-POC. Note that these weights are derived according to the expert agent’s policy. From the first transition executed by a random policy to the last transition executed by the expert agent, the sampled batches become on-policy with respect to the trained agent’s policy. We observe that as the center of the sliding window approaches the last transition, the AC-Off-POC weights approach the value 1. Hence, the weights increases as the on-policyness of the sampled batch increases, which we observe from the linear path taken by the AC-Off-POC weights. Overall, we infer that the deterministic variant of the AC-Off-POC produces accurate estimates with negligible error. However, it does not employ temporally correlated trajectories or any action probability estimate.

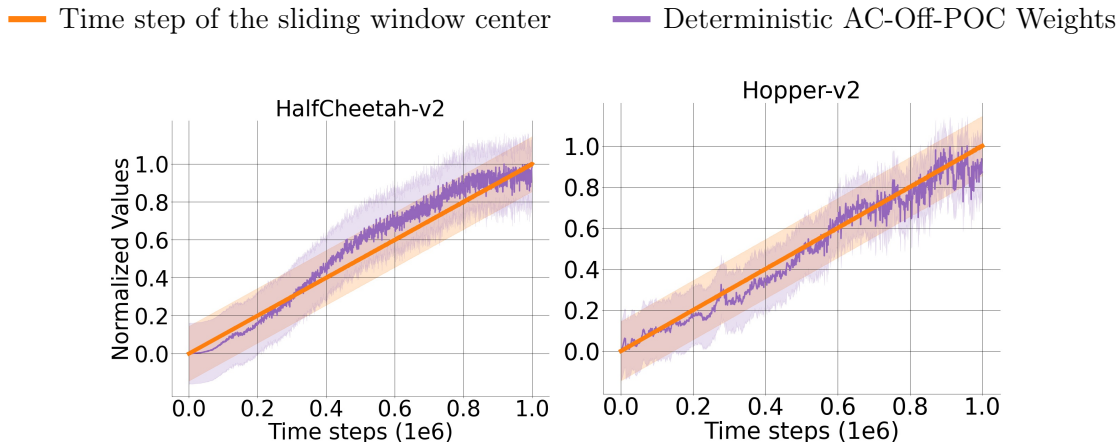


Figure 4: Temporally ordered batches of transitions versus similarity weights produced by deterministic AC-Off-POC under the TD3 algorithm for the set of OpenAI Gym continuous control tasks over 1 million training time steps. The shaded region represents a 95% confidence interval of the normalized values over the trials.

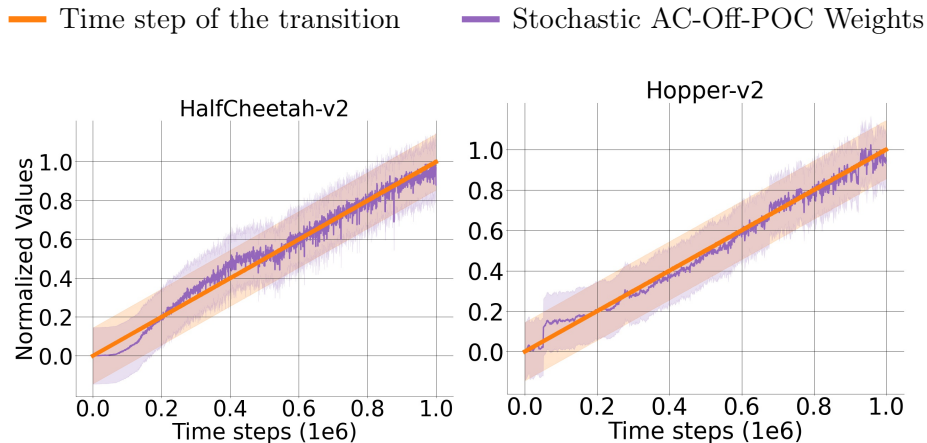


Figure 5: Temporally ordered transitions versus similarity weights produced by stochastic AC-Off-POC under the SAC algorithm for the set of OpenAI Gym continuous control tasks over 1 million training time steps. The shaded region represents a 95% confidence interval of the normalized values over the trials.

We conduct the same set of experiments to verify the accuracy of the stochastic variant of AC-Off-POC. As the stochastic variant assigns unique weights to each off-policy sample, we directly depict the weights assigned to each transition contained in the expert agent’s experience replay buffer. In Figure 5, we observe that the stochastic variant also produces accurate similarity weights to schedule the contribution of each loss component with respect to off-policy samples. Moreover, the confidence of the weights is more robust, and weights are more accurate due to the direct use of the policy distributions in computing the dissimilarity between the target and behavioral policies. In conclusion, as discussed in Remark 5, AC-Off-POC can produce accurate similarity weights by preventing vanishing or exploding gradients and the employment of trajectories due to the transition-wise or temporally uncorrelated batch-wise similarities.

## 6. Conclusion

In this paper, we discuss the theme of off-policy correction, which mitigates the potential effects of off-policy samples whose underlying distribution is divergent from the current policy of interest. As the action probabilities cannot be known and estimated, off-policy correction through eligibility traces for deterministic policies is not available in continuous control. To make the actor-critic methods closer to their on-policy nature, we introduce a novel off-policy correction approach with two variants for stochastic and deterministic policies, AC-Off-POC, which achieves an efficient single-step off-policy correction, enables a safe off-policy learning and, improves the data-efficiency by reweighting the contribution of off-policy samples to the loss of the value function and policy. We support our claims with solid theoretical analysis

that the introduced off-policy correction schemes obtain a bounded contraction mapping which enables a safe single-step off-policy correction.

An extensive set of empirical studies shows that AC-Off-POC improves the state-of-the-art and outperforms the competing off-policy correction methods by a considerable margin. By overcoming the bias induced by the off-policy samples contained in the experience replay buffer, our method can attain faster convergence and optimal policies by disregarding the transitions executed by behavioral policies that highly deviate from the current policy of the numerical action decisions. Our method also resolves computational cost issues by not introducing hyper-parameters or networks. Furthermore, we support our remarks with experimental results throughout the paper. We show that a generic approach can readily apply AC-Off-POC to any off-policy actor-critic method. Lastly, we provide an open-source repository<sup>1</sup> containing all the code and results to further support research on off-policy deep RL.

## Appendix A. Proof of Lemma 7

**Lemma 7** *The difference between  $\mathcal{H}Q$  and its fixed point  $Q^\pi$  is:*

$$\mathcal{H}Q(s, a) - Q^\pi(s, a) = \gamma \mathbb{E}_{s \sim P_\eta, a \sim \eta} [\mathbb{E}_\pi [(Q - Q^\pi)(s, \cdot)] - \lambda(Q - Q^\pi)(s, a)].$$

**Proof** The proof reduces the proof of Lemma 1 by Munos et al. (2016) to single-step TD-learning when off-policy correction is involved. First, rewrite Equation 14 in terms of the next state-action pair:

$$\mathcal{H}Q(s, a) = \mathbb{E}_\eta [\lambda (r + \gamma (\mathbb{E}_\pi Q(s', \cdot) - \lambda' Q(s', a')))].$$

As  $Q^\pi$  is the fixed point of  $\mathcal{H}$ , we have:

$$Q^\pi(s, a) = \mathcal{H}Q^\pi(s, a) = \mathbb{E}_\eta [\lambda (r + \gamma (\mathbb{E}_\pi Q^\pi(s', \cdot) - \lambda' Q^\pi(s', a')))].$$

Letting  $\Delta Q := Q - Q^\pi$ , we infer that:

$$\mathcal{H}Q(s, a) - Q^\pi(s, a) = \mathbb{E}_\eta [\lambda \gamma (\mathbb{E}_\pi \Delta Q(s', \cdot) - \lambda' \Delta Q(s', a))].$$

Decrementing the bootstrapping by a single step:

$$\mathcal{H}Q(s, a) - Q^\pi(s, a) = \gamma \mathbb{E}_{s \sim P_\eta, a \sim \eta} [\mathbb{E}_\pi \Delta Q(s, \cdot) - \lambda \Delta Q(s, a)],$$

where  $\gamma$  can be taken out of the expectation operator since it is fixed. ■

## References

- Richard Bellman. *Dynamic Programming*. Dover Publications, 1957. ISBN 9780486428093.
- D. P. Bertsekas and J. N. Tsitsiklis. *Neuro-dynamic programming*. Athena Scientific, Belmont, MA, 1996.
- Greg Brockman, Vicki Cheung, Ludwig Pettersson, Jonas Schneider, John Schulman, Jie Tang, and Wojciech Zaremba. Openai gym. *CoRR*, abs/1606.01540, 2016. URL <http://arxiv.org/abs/1606.01540>.
- Dogan C. Cicek, Enes Duran, Baturay Saglam, Furkan B. Mutlu, and Suleyman S. Kozat. Off-policy correction for deep deterministic policy gradient algorithms via batch prioritized experience replay. In *2021 IEEE 33rd International Conference on Tools with Artificial Intelligence (ICTAI)*, pages 1255–1262, 2021. doi: 10.1109/ICTAI52525.2021.00199.
- Christoph Dann, Gerhard Neumann, and Jan Peters. Policy evaluation with temporal differences: A survey and comparison. *Journal of Machine Learning Research*, 15(24): 809–883, 2014. URL <http://jmlr.org/papers/v15/dann14a.html>.
- Tim de Bruin, Jens Kober, Karl Tuyls, and Robert Babuška. Experience selection in deep reinforcement learning for control. *Journal of Machine Learning Research*, 19(9):1–56, 2018. URL <http://jmlr.org/papers/v19/17-131.html>.

- Thomas Degris, Martha White, and Richard S. Sutton. Off-policy actor-critic. In *Proceedings of the 29th International Conference on Machine Learning*, ICML'12, page 179–186, Madison, WI, USA, 2012. Omnipress. ISBN 9781450312851.
- Lasse Espeholt, Hubert Soyer, Remi Munos, Karen Simonyan, Vlad Mnih, Tom Ward, Yotam Doron, Vlad Firoiu, Tim Harley, Iain Dunning, Shane Legg, and Koray Kavukcuoglu. IMPALA: Scalable distributed deep-RL with importance weighted actor-learner architectures. In Jennifer Dy and Andreas Krause, editors, *Proceedings of the 35th International Conference on Machine Learning*, volume 80 of *Proceedings of Machine Learning Research*, pages 1407–1416. PMLR, 10–15 Jul 2018. URL <https://proceedings.mlr.press/v80/espeholt18a.html>.
- Scott Fujimoto, Herke van Hoof, and David Meger. Addressing function approximation error in actor-critic methods. In Jennifer Dy and Andreas Krause, editors, *Proceedings of the 35th International Conference on Machine Learning*, volume 80 of *Proceedings of Machine Learning Research*, pages 1587–1596. PMLR, 10–15 Jul 2018. URL <https://proceedings.mlr.press/v80/fujimoto18a.html>.
- Scott Fujimoto, David Meger, and Doina Precup. Off-policy deep reinforcement learning without exploration. In Kamalika Chaudhuri and Ruslan Salakhutdinov, editors, *Proceedings of the 36th International Conference on Machine Learning*, volume 97 of *Proceedings of Machine Learning Research*, pages 2052–2062. PMLR, 09–15 Jun 2019. URL <https://proceedings.mlr.press/v97/fujimoto19a.html>.
- Matthieu Geist and Bruno Scherrer. Off-policy learning with eligibility traces: A survey. *Journal of Machine Learning Research*, 15(10):289–333, 2014. URL <http://jmlr.org/papers/v15/geist14a.html>.
- Shixiang (Shane) Gu, Timothy Lillicrap, Richard E Turner, Zoubin Ghahramani, Bernhard Schölkopf, and Sergey Levine. Interpolated policy gradient: Merging on-policy and off-policy gradient estimation for deep reinforcement learning. In I. Guyon, U. Von Luxburg, S. Bengio, H. Wallach, R. Fergus, S. Vishwanathan, and R. Garnett, editors, *Advances in Neural Information Processing Systems*, volume 30. Curran Associates, Inc., 2017. URL <https://proceedings.neurips.cc/paper/2017/file/a1d7311f2a312426d710e1c617fcbc8c-Paper.pdf>.
- Tuomas Haarnoja, Aurick Zhou, Pieter Abbeel, and Sergey Levine. Soft actor-critic: Off-policy maximum entropy deep reinforcement learning with a stochastic actor. In Jennifer Dy and Andreas Krause, editors, *Proceedings of the 35th International Conference on Machine Learning*, volume 80 of *Proceedings of Machine Learning Research*, pages 1861–1870. PMLR, 10–15 Jul 2018. URL <https://proceedings.mlr.press/v80/haarnoja18b.html>.
- Seungyul Han and Youngchul Sung. Dimension-wise importance sampling weight clipping for sample-efficient reinforcement learning. In Kamalika Chaudhuri and Ruslan Salakhutdinov, editors, *Proceedings of the 36th International Conference on Machine Learning*, volume 97 of *Proceedings of Machine Learning Research*, pages 2586–2595. PMLR, 09–15 Jun 2019. URL <https://proceedings.mlr.press/v97/han19b.html>.

- Anna Harutyunyan, Marc G. Bellemare, Tom Stepleton, and Rémi Munos.  $Q(\lambda)$  with off-policy corrections. In *ALT*, pages 305–320, 2016. URL [https://doi.org/10.1007/978-3-319-46379-7\\_21](https://doi.org/10.1007/978-3-319-46379-7_21).
- Peter Henderson, Riashat Islam, Philip Bachman, Joelle Pineau, Doina Precup, and David Meger. Deep reinforcement learning that matters. *Proceedings of the AAAI Conference on Artificial Intelligence*, 32(1), Apr. 2018. URL <https://ojs.aaai.org/index.php/AAAI/article/view/11694>.
- Mahammad Humayoo and Xueqi Cheng. Relative importance sampling for off-policy actor-critic in deep reinforcement learning, 2019.
- Ehsan Imani, Eric Graves, and Martha White. An off-policy policy gradient theorem using emphatic weightings. In S. Bengio, H. Wallach, H. Larochelle, K. Grauman, N. Cesa-Bianchi, and R. Garnett, editors, *Advances in Neural Information Processing Systems*, volume 31. Curran Associates, Inc., 2018. URL <https://proceedings.neurips.cc/paper/2018/file/3ef815416f775098fe977004015c6193-Paper.pdf>.
- Timothy P. Lillicrap, Jonathan J. Hunt, Alexander Pritzel, Nicolas Heess, Tom Erez, Yuval Tassa, David Silver, and Daan Wierstra. Continuous control with deep reinforcement learning. In *ICLR (Poster)*, 2016. URL <http://arxiv.org/abs/1509.02971>.
- Long-Ji Lin. Self-improving reactive agents based on reinforcement learning, planning and teaching. *Machine Learning*, 8(3):293–321, May 1992. ISSN 1573-0565. doi: 10.1007/BF00992699. URL <https://doi.org/10.1007/BF00992699>.
- A. Mahmood, H. V. Hasselt, and R. Sutton. Weighted importance sampling for off-policy learning with linear function approximation. In *NIPS*, 2014.
- Alberto Maria Metelli, Matteo Papini, Francesco Faccio, and Marcello Restelli. Policy optimization via importance sampling. In S. Bengio, H. Wallach, H. Larochelle, K. Grauman, N. Cesa-Bianchi, and R. Garnett, editors, *Advances in Neural Information Processing Systems*, volume 31. Curran Associates, Inc., 2018. URL <https://proceedings.neurips.cc/paper/2018/file/6aed000af86a084f9cb0264161e29dd3-Paper.pdf>.
- Alberto Maria Metelli, Matteo Papini, Nico Montali, and Marcello Restelli. Importance sampling techniques for policy optimization. *Journal of Machine Learning Research*, 21(141):1–75, 2020. URL <http://jmlr.org/papers/v21/20-124.html>.
- Remi Munos, Tom Stepleton, Anna Harutyunyan, and Marc Bellemare. Safe and efficient off-policy reinforcement learning. In D. Lee, M. Sugiyama, U. Luxburg, I. Guyon, and R. Garnett, editors, *Advances in Neural Information Processing Systems*, volume 29. Curran Associates, Inc., 2016. URL <https://proceedings.neurips.cc/paper/2016/file/c3992e9a68c5ae12bd18488bc579b30d-Paper.pdf>.
- Ian Parberry. *Introduction to Game Physics with Box2D*. CRC Press, Inc., USA, 1st edition, 2013. ISBN 1466565764.
- Doina Precup, Richard Sutton, and Satinder Singh. Eligibility traces for off-policy policy evaluation. *Computer Science Department Faculty Publication Series*, 06 2000.

- Doina Precup, Richard Sutton, and Sanjoy Dasgupta. Off-policy temporal-difference learning with function approximation. *Proceedings of the 18th International Conference on Machine Learning*, 06 2001.
- Antonin Raffin. Rl baselines3 zoo. <https://github.com/DLR-RM/rl-baselines3-zoo>, 2020.
- Baturay Saglam, Dogan C. Cicek, Furkan B. Mutlu, and Suleyman S. Kozat. Safe and robust experience sharing for deterministic policy gradient algorithms, 2022a. URL <https://arxiv.org/abs/2207.13453>.
- Baturay Saglam, Furkan B. Mutlu, Dogan C. Cicek, and Suleyman S. Kozat. Actor prioritized experience replay, 2022b. URL <https://arxiv.org/abs/2209.00532>.
- Tom Schaul, John Quan, Ioannis Antonoglou, and David Silver. Prioritized experience replay. In *ICLR (Poster)*, 2016. URL <http://arxiv.org/abs/1511.05952>.
- Simon Schmitt, Matteo Hessel, and Karen Simonyan. Off-policy actor-critic with shared experience replay. In Hal Daumé III and Aarti Singh, editors, *Proceedings of the 37th International Conference on Machine Learning*, volume 119 of *Proceedings of Machine Learning Research*, pages 8545–8554. PMLR, 13–18 Jul 2020. URL <https://proceedings.mlr.press/v119/schmitt20a.html>.
- Richard Sutton. Learning to predict by the method of temporal differences. *Machine Learning*, 3:9–44, 08 1988a. doi: 10.1007/BF00115009.
- Richard S. Sutton. Learning to predict by the methods of temporal differences. *Machine Learning*, 3(1):9–44, Aug 1988b. ISSN 1573-0565. doi: 10.1007/BF00115009. URL <https://doi.org/10.1007/BF00115009>.
- Richard S Sutton and Andrew G Barto. *Reinforcement learning: An introduction*. MIT press, 2018.
- Richard S. Sutton, A. Rupam Mahmood, and Martha White. An emphatic approach to the problem of off-policy temporal-difference learning. *Journal of Machine Learning Research*, 17(73):1–29, 2016. URL <http://jmlr.org/papers/v17/14-488.html>.
- E. Todorov, T. Erez, and Y. Tassa. Mujoco: A physics engine for model-based control. In *2012 IEEE/RSJ International Conference on Intelligent Robots and Systems*, pages 5026–5033, 2012. doi: 10.1109/IROS.2012.6386109.
- Christopher Watkins. Learning from delayed rewards, 01 1989.
- Christopher J. C. H. Watkins and Peter Dayan. Q-learning. *Machine Learning*, 8(3):279–292, May 1992. ISSN 1573-0565. doi: 10.1007/BF00992698. URL <https://doi.org/10.1007/BF00992698>.
- R. J. Williams. Simple statistical gradient-following algorithms for connectionist reinforcement learning. *Machine Learning*, 8:229–256, 1992.

- Huizhen Yu, A. Rupam Mahmood, and Richard S. Sutton. On generalized bellman equations and temporal-difference learning. *Journal of Machine Learning Research*, 19(48):1–49, 2018. URL <http://jmlr.org/papers/v19/17-283.html>.
- Daochen Zha, Kwei-Herng Lai, Kaixiong Zhou, and Xia Hu. Experience replay optimization. In *Proceedings of the Twenty-Eighth International Joint Conference on Artificial Intelligence, IJCAI-19*, pages 4243–4249. International Joint Conferences on Artificial Intelligence Organization, 7 2019. doi: 10.24963/ijcai.2019/589. URL <https://doi.org/10.24963/ijcai.2019/589>.
- Shangdong Zhang and Richard S Sutton. A deeper look at experience replay. *arXiv preprint arXiv:1712.01275*, 2017.
- Shangdong Zhang and Shimon Whiteson. Truncated emphatic temporal difference methods for prediction and control. *Journal of Machine Learning Research*, 23(153):1–59, 2022. URL <http://jmlr.org/papers/v23/21-0934.html>.
- Shangdong Zhang, Wendelin Boehmer, and Shimon Whiteson. Generalized off-policy actor-critic. In H. Wallach, H. Larochelle, A. Beygelzimer, F. d'Alché-Buc, E. Fox, and R. Garnett, editors, *Advances in Neural Information Processing Systems*, volume 32. Curran Associates, Inc., 2019. URL <https://proceedings.neurips.cc/paper/2019/file/0e095e054ee94774d6a496099eb1cf6a-Paper.pdf>.